2010 Ohio UTC Student Research Conference

Abstract Summaries

November 12, 2010

The University of Akron Student Union

Akron, Ohio

Acknowledgements

Sponsors:

Ohio Transportation Consortium, Dr. Ping Yi, Director
The University of Akron
Akron, Ohio 44325-6106
330-972-6543
330-972-5449 (fax)
otc@uakron.edu
www.otc.uakron.edu

Center for Transportation and Materials Engineering, Joann Esenwein, Director
Youngstown State University
Moser Hall 2055
Youngstown, Ohio 44555
330-941-2421
ctme@ysu.edu
http://stem.ysu.edu/CTME

Intermodal Transportation Institute, Richard Martinko, P.E., Director
The University of Toledo
Research and Technology Complex - R1
2801 W. Bancroft Street, Mail Stop 218
Toledo, OH 43606-3390
419-530-5221
419-530-7246 (fax)
www.utoledo.edu/research/iti

University Transportation Center - Cleveland State University, Dr. Stephen Duffy, Director
Fenn College of Engineering
Cleveland State University
2121 Euclid Ave. SH 107
Cleveland, Ohio 44115-2214
216-687-3874
216-687-5395 (fax)
S.duffy@csuohio.edu
www.csuohio.edu/engineering/utc

Contents

Bicycle-Sharing in a College Environment

Megan Petroski,
Graduate Student, Kent State University

Abstract Summary

Bike sharing is an effective way of providing access to sustainable modes of transportation to a large population. This stems from a desire by the campus community to begin a bike-sharing program that moves students, faculty, staff, and community members from one place to another. Current transportation patterns on the Kent State University campus and within the city of Kent demonstrate that bike-sharing has a great deal of potential. Based on a web survey administered last year, about 60% of Kent State University students do not have access to working bikes. This represents a large population of potential users. To address this issue, Kent State recently began a pilot program – FlashFleet - with fifty bikes in six locations around campus. Our efforts are now focused on expanding the program to meet this demand as well as to move towards an automated system which would make checking bicycles out more convenient for users.

This presentation reports on the viability of expanding a bike sharing program on the Kent campus based on current and future transportation demands and the potential to widening the pilot programs' scope. First, I examine the nature of potential demand for bike-sharing, based around survey and focus group information. Then, I use surveys taken by FlashFleet users to analyze where they went on the bike and the nature of their experience. Finally, I assess the state of bike-sharing programs in campuses across the country as a way to determine the best method of expanding this bike sharing program at the lowest cost.

Comparison of Advance Dilemma Zone Protection Algorithms

Sai Geetha.K
Graduate Student, Department of Civil Engineering, University of Akron

Abstract

High speed signalized intersections involve some safety problems in addition to operation and design issues. One of the most important safety problems at the high speed intersection is dilemma zone protection. Dilemma zone come into existence when the vehicle is approaching the intersection at the end of the green phase. The advance dilemma zone protection system increases the safety at the intersection by changing traffic timing to reduce the number of vehicles entering the dilemma zone. This may reduce rare end and angle crashes at the intersection.

Introduction

The yellow phase dilemma is one of the major contributing factors to intersection related crashes, particularly the rear end and right angle crashes. The so called dilemma is reflective to drivers' indecisiveness when making stop/pass decisions in response to yellow indications. This dilemma is usually characterized by a physical zone in advance of the intersection, which is termed as dilemma zone (DZ). The concept of dilemma zone was initially proposed by Gazis et al. as a roadway segment within which a vehicle approaching an intersection during the yellow interval can neither safely clear the intersection, nor comfortably stop before the stop line.

A driver approaching a signalized intersection as the light turns yellow will either have to stop or proceed through the intersection. If the driver decided to stop, the distance required to safely stop before entering the intersection is known as the stop zone (represented by X_s, in the figure below) and is defined as $$Stop\ Zone = vt + \frac{v^2}{2g(f \pm G)}$$

where:

v = vehicle approach speed (ft/sec)

t = driver perception reaction time (sec)

g = acceleration of gravity (ft/sec2)

f = coefficient of friction

G = roadway gradient (%/100)

From the onset of the yellow interval, the distance a vehicle must travel with no change in speed and be able to safely proceed through the intersection is known as the go zone (represented by X_c in the figure below) and is formulated as follows:

$$Go\ Zone = yv - (W + L)$$

where:

y = yellow interval (sec)

V = vehicle approach speed (ft/sec)

W = intersection width (ft)

L = length of vehicle (ft)

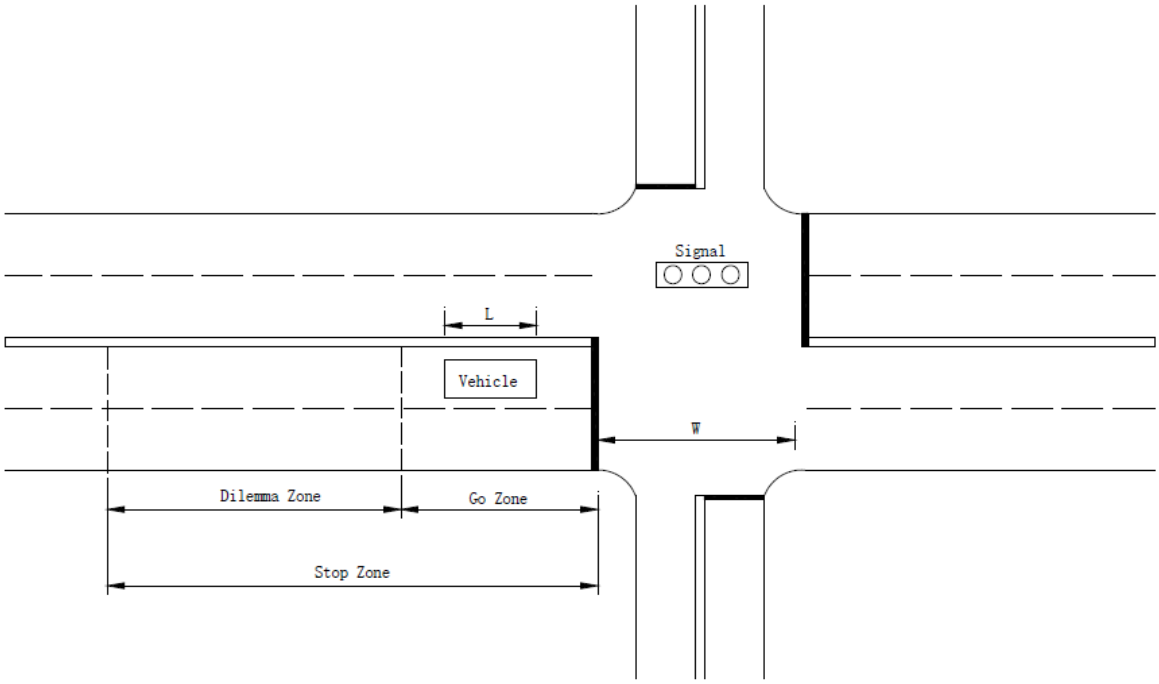

Fig.1.1 Dilemma Zone at an intersection

The dilemma zone, which is the segment of road on approach to an intersection where a vehicle's location within it creates indecision for drivers with regard to stopping or proceeding, is given by:

Dilemma Zone **= Stop Zone – Go Zone**

Algorithm for Dilemma Zone Protection

This algorithm firstly calculates the stop zone and go zone for all the vehicles approaching an intersection on the main approach. The process of checking the vehicle in dilemma zone occur every 0.2 second interval and starts at a distance of 1000 feet from the stop line. Once the vehicle is

confirmed that it will be in dilemma zone in 1 second, the green signal is extended by 1 second to protect this vehicle as it enters. The extension described above occurs only when there is a conflicting call from the minor approach. This algorithm checks the nearest vehicle to stop line, to see if it is in Dilemma Zone or not, and extends green accordingly. This algorithm terminates the green only if, there is no vehicle in the dilemma zone or if max-out occurs.

FLOWCHART 80%-20% DZ

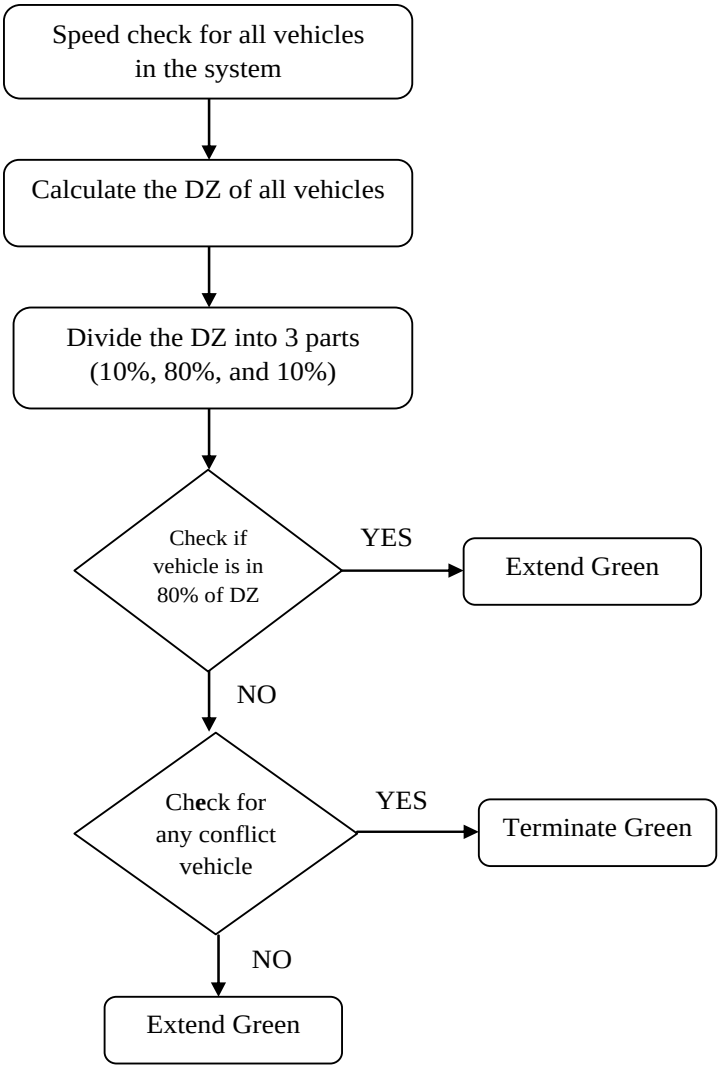

Explanation of flow chart

Step 1: For Dilemma Zone protection, this algorithm firstly calculates the stop zone and go zone for all the vehicles approaching an intersection on the main approach and calculates the dilemma zone for each vehicle.

Step 2: Now the dilemma zone is divided into three parts 10%, 80% and 10%. This process of checking

the vehicle in dilemma zone occur every 0.2sec interval and starts at a distance of 1000 feet from the stop line

Step 3: The system first checks if the vehicle is in the 80% of the dilemma zone,

(i) If **"yes"** it will extend green.

(ii) If **"no",** then the system again checks for any conflict call from the other approach .If there is any conflict call then it terminates green or else extend green.

This algorithm checks the nearest vehicle to stop line, to see if it is in Dilemma Zone or not, and extends green accordingly.

FLOWCHART 50%-75% DZ

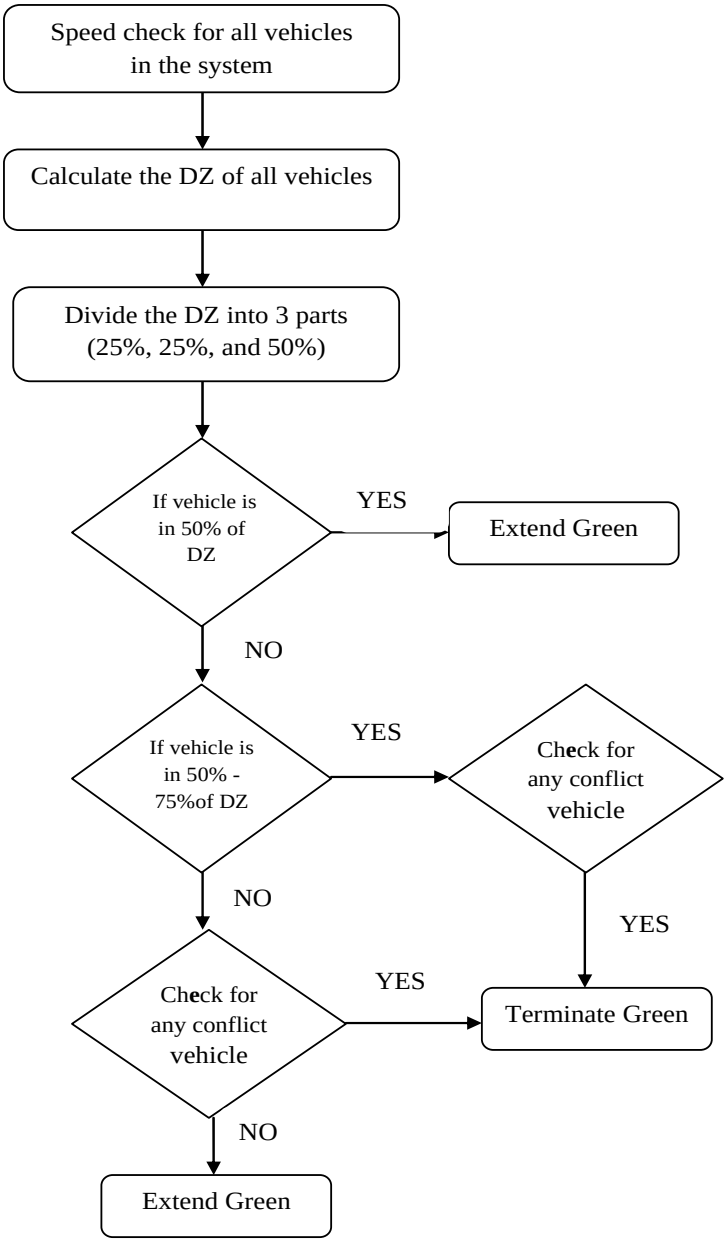

Explanation of flow chart

Step 1: For Dilemma Zone protection, this algorithm firstly calculates the stop zone and go zone for all the vehicles approaching an intersection on the main approach and calculates the dilemma zone for each vehicle.

Step 2: Now the dilemma zone is divided into three parts 25%, 25% and 50%. This process of checking the vehicle in dilemma zone occur every 0.2 sec interval and starts at a distance of 1000 feet from the stop line

Step 3: The system first checks if the vehicle is in the 50% of the dilemma zone,

(i) If "yes" it will extend green.

(ii) If "no" then the system will again check if there is any vehicle in the 50-75% of the dilemma zone.

(a) If **"yes"** then it will check if there is any conflict calls from the other approach, if vehicle is present then it will terminate green or else extend green.

(b) If **"no",** then the system again checks for any conflict call from the other approach .If there is any conflict call then it terminates green or else extend green.

This algorithm checks the nearest vehicle to stop line, to see if it is in Dilemma Zone or not, and extends green accordingly.

Comparison between the 50-75% Dilemma Zone and 20-80% Dilemma Zone Algorithm

For comparing these two advance dilemma zone protection algorithms, an intersection was drawn in VISSIM (having major and minor road). The following combination of the volumes for major and minor were used for various simulation runs:

Volume Major Road	Volume Minor Road
300	400
600	400
900	400
1200	400
300	200
600	200
900	200
1200	200

Results

The number of extensions of green interval was the bases of comparison between the algorithms. After running the simulations for 550 simulation-second, the following results were obtained as the number of extensions and total delay for different volume combinations on major and minor roads:

10-80% DZ Algorithm			
Volume Major Road	Volume Minor Road	Extension	Delay
300	400	4	422.915
600	400	10	95.153
900	400	22	242.067
1200	400	29	475.75

Volume Major Road	Volume Minor Road	Extension	Delay
300	200	2	77.95
600	200	8	119.665
900	200	13	140.119
1200	200	13	250.139

50-75% DZ Algorithm			
Volume Major Road	Volume Minor Road	Extension	Delay
300	400	4	100.86
600	400	7	35.8731
900	400	9	96.838
1200	400	4	25.299

Volume Major Road	Volume Minor Road	Extension	Delay
300	200	2	60.95
600	200	7	34.057
900	200	9	33.794
1200	200	10	55.265

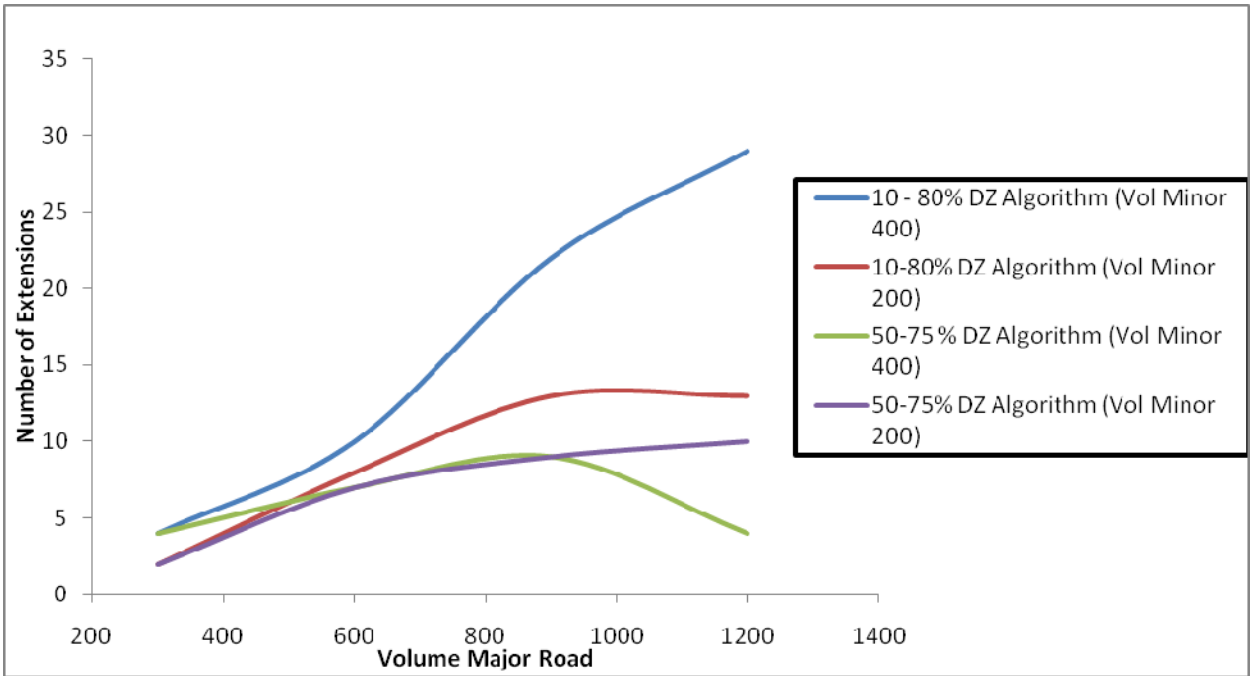

Fig. 1.2 Comparison of number of extensions for two algorithms having different volume combinations

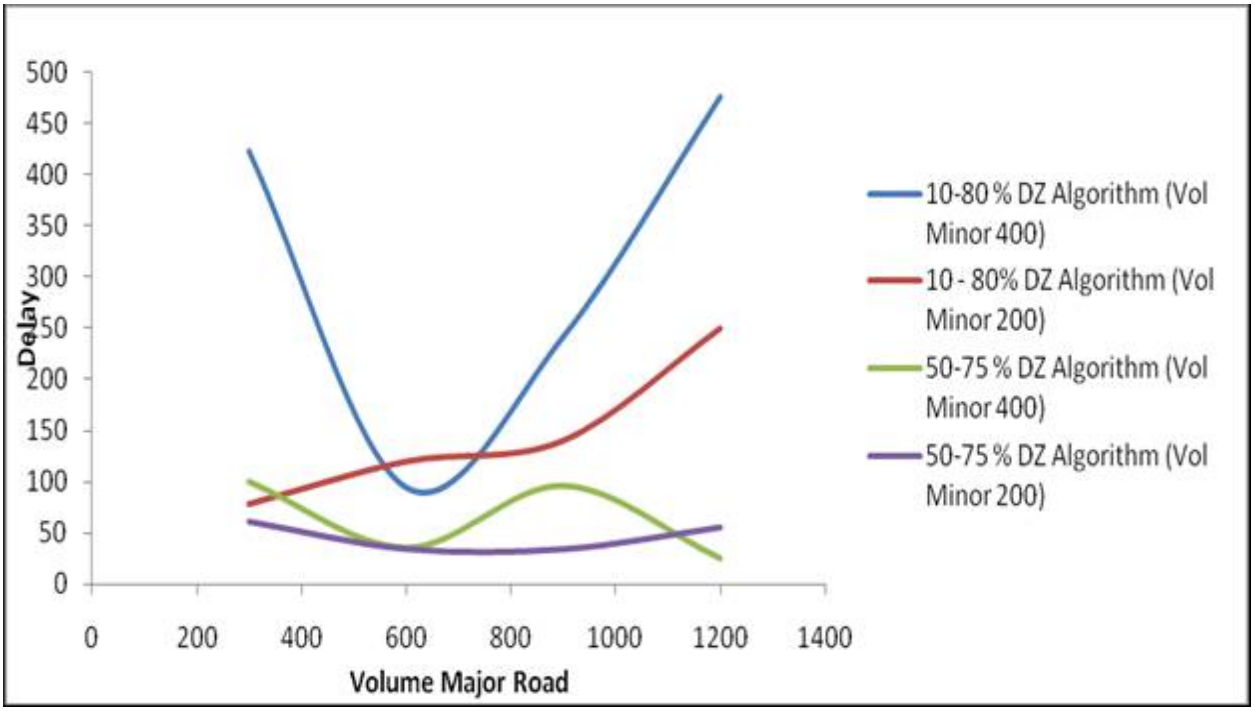

Fig. 1.3 Comparison of delay for two algorithms having different volume combinations

Conclusion

It's quite evident from the Fig .1.2 above that there is difference between numbers of extensions in both the cases. The number of extensions in 10-80% algorithm is much higher as compared to 50-75% algorithm, when volume on major road is increased. This may be due to reason that in 10-80% algorithm, the Dilemma Zone is shortened by 20 % whereas in 50-75% algorithm the last 25 % of Dilemma Zone is always neglected for extensions i.e. dilemma zone is always shortened for 25% or more. Hence, less number of vehicles falls in shortened dilemma zone for which extension can occur.

Fig. 1.3 shows that there is no relationship between the volume on major road and delay, this may be because of the reason that simulations ran with combination of volume (major and minor road volume) were just ran for one time and that too for small time period of 550 simulation-seconds.

Causes of Bumps at Pavement-Bridge Interface

AKM Anwarul Islam, PhD., P.E.
Associate Professor, Civil & Environmental Engineering, Youngstown State University

Amar Shukla
Graduate Student, Civil & Environmental Engineering, Youngstown State University,

Summary

This research was performed to determine the probable causes and cost-effective solutions for reducing bumps at pavement-bridge interface. Bumps can be defined as the differential settlement between a bridge and an approach slab. Approach slabs are provided for better transition of vehicles. Briaud et al. (1997) summarized that out of 600,000 bridges across the United States; approximately 150,000 bridges have bumps that cost approximately $100 million annually for repair. Bumps not only cause discomforts to riders but also create bad images of transportation departments.

A thorough study of previous research work were conducted and various causes of bumps were found, which were: movement of soil beneath the slab, strength deficient approach slabs, continual impact of vehicles running over already compacted area, insufficient compaction of soil especially of the embankment backfill, types of soil, short-term and long-term settlement, bridge end conditions, construction methods, roadway paving and bridge/roadway joint, water seepage and traffic volume.

This research was based on two major causes of bridge bumps which are movement/settlement of soil under the approach slab and insufficient strength of an approach slab. Experimental investigations were conducted on 2 bridges with bumps and 3 bridges without bumps at Columbiana County in Ohio. Soil was collected from the surface and Sieve Analysis tests and Atterberg Limit tests (Liquid Limit and Plastic Limit) were performed. Soil was classified according to AASHTO Standards as shown in Table 1.1. It was found that the soil is granular for all the sites and various methods through which proper compaction of granular soil can be obtained are pneumatic rubber-tired rollers, vibratory rollers and handheld vibrating plates.

Standard drawings of different State Departments of Transportation (DOTs) were studied and respective strengths of approach slabs of those DOTs were determined as shown in Table 1.2. For calculations slab was considered as doubly reinforced and simply supported.

Finite element analysis of Ohio approach slab was performed by building 2 different models of approach slab in ALGOR. First model was built considering the soil is underneath the approach slab while the second model was built considering all the soil has moved out underneath the approach slab, as shown in Fig. 1.1 and 1.2, respectively. The geometric parameters for both approach slabs were:

- Length = 30 ft.; Width = 20 ft.
- Bottom Steel - #10 reinforcing bars @ 6.5 in. c.c.
- Top Steel and Bent Steel - # 5 reinforcing bars @ 18 in. c.c.
- Vertical Steel - #5 reinforcing bars @ 6 in. c.c.

Table 1.1 – AASHTO Soil Classification of different soil samples

Results on	Bridges without bumps		Bridges with bumps		
	COL 30 2578	COL 30 2667	COL 30 11 2L	COL 30 2670	COL 30 3182
Liquid Limit	34.1	21.5	24.9	33.6	32.2
Plastic Limit	24.5	25.5	21.9	30.7	38.4
Plasticity Index	9.6	NP	3.4	2.9	NP
Soil Classification	A-2-4 (0)	A-3 (0)	A-1-b (0)	A-1-b (0)	A-3 (0)

Table 1.2 - Approach Slab Designs in different state DOTs

State	L_{min} (ft.)	h (in.)	$f_{c'}$ (ksi)	A_s (in^2/ ft)	$A_{s'}$ (in^2/ ft)	d' (in.)	C_c (in.)	ΦM_n (kip*ft/ ft)	M_u (kip*ft/ ft)
AZ	15	12	3	1.053	0.133	2.5	3	37.57	9.77
FL*	30	12	4.5	1.053	0.310	2.5	4	31.05	80.03
IN	20	10	4	0.630	0.203	2.5	2	19.14	30.16
KY	25	17	3.5	1.580	0	NP	3	90.10	61.72
MI*	20	12	4.5	0.895	0.895	3	3	21.87	31.72
OH	30	17	4.5	2.345	0.207	3	3	129.81	90.40
PA	25	16	3.5	1.693	0.310	2.5	3	85.22	60.50

* denotes that applied moment is more than internal moment capacity; NP means Not Provided

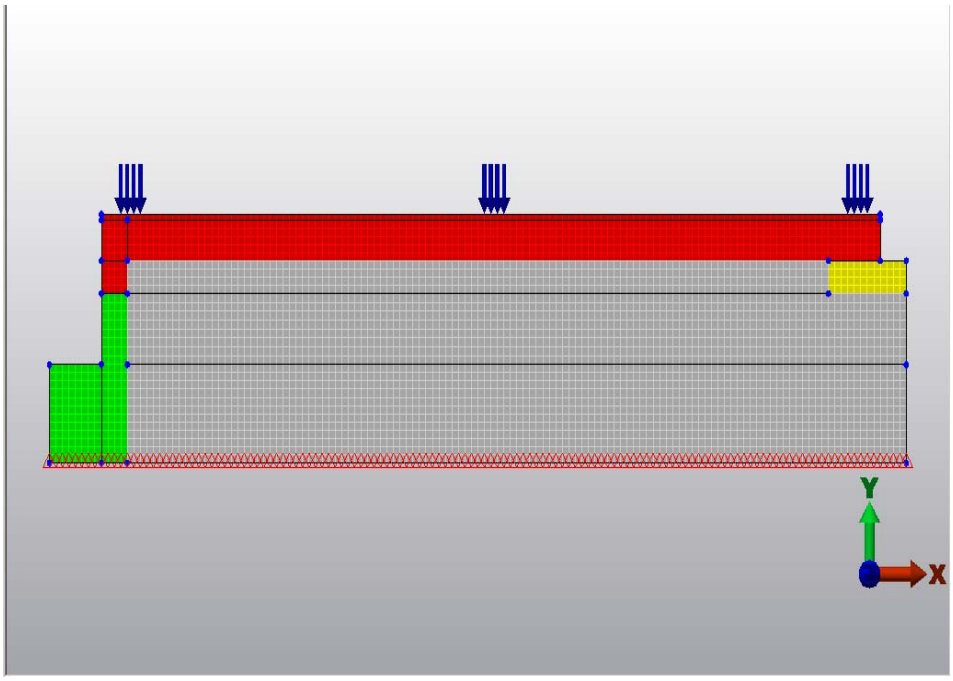

Figure 1.1 - FEM of approach slab with soil underneath

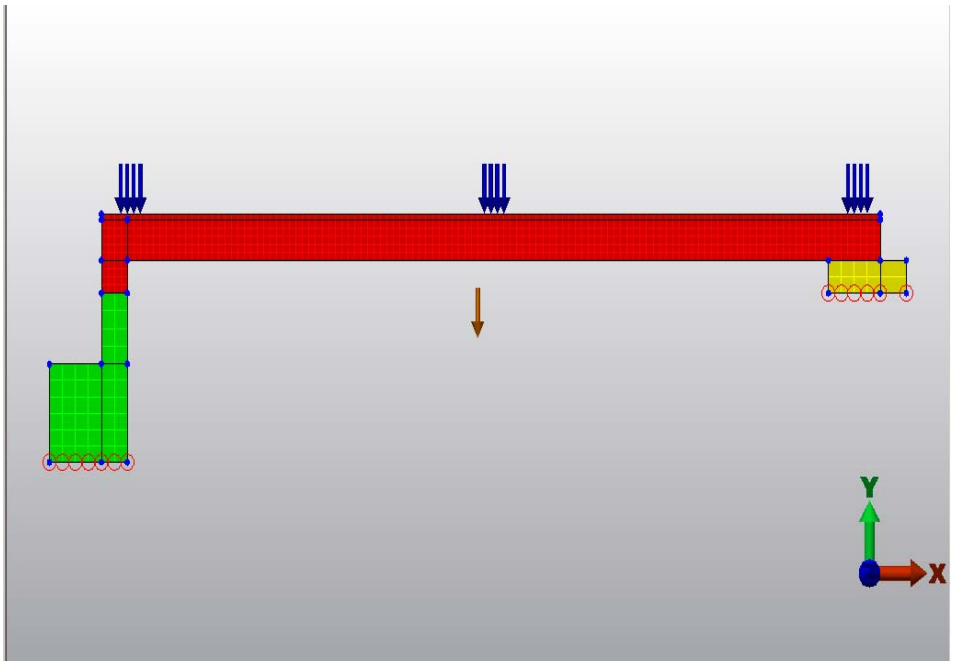

Figure 1.2 - FEM of approach slab without soil

The model in Fig. 1.1 is fixed while the model in Fig. 1.2 is simple supported. The worst loading scenario of HL-93 truck single lane loading conditions was considered. Contact between approach slab and end was considered as bonded while the contact between approach slab and sleeper slab was considered as a surface contact. The value of coefficient of static friction between concrete was taken

as 0.75. Analysis on both the models was performed and it was found that the deflection roughly increases by 3 times and beam stress increases by 5 times when soil moves out underneath the approach slab. The results obtained for both the models are shown in Table 1.3.

Table 1.3 – FEM Analysis results for both models

Model	Deflection (in.)	Maximum Beam Stress (lb/in^2)
Soil underneath	0.057	569.245
No soil underneath	0.179	3028.978

Calculations were performed using the maximum beam stress value obtained from the model when soil completely moves out underneath the approach slab and applied moment was calculated, M_u = 139.95 kip-ft. which was more than the internal moment capacity (ΦM_n = 128.91 kip-ft.) used by Ohio Department of Transportation. Thus the slab was redesigned and the recommendations are given below:

- Length = 30 ft.; Width = 20 ft.
- Bottom reinforcement - #10 @ 5.5 in. c.c.
- Top reinforcement - #5 @ 18 in. c.c.

References

American Association of State Highway and Transportation Officials, LRFD Bridge Design Specifications, 4th edition, 2007.

Briaud, J. L., James, R. W., and Hoffman, S. B. (1997). NCHRP synthesis 234: "Settlement of Bridge Approaches (the bump at the end of the bridge)," Transportation Research Board, National Research Council, Washington, D.C., 75 pp.

Cai, C.S., Voyiadjis, G.Z., and Shi, X. (2005). "Determination of Interaction between Bridge Concrete Approach Slab and Embankment Settlement," Report No. FHWA/LA. 05/403, Louisiana Transportation Research Center, Louisiana Department of transportation, 152 pp.

Safety Evaluation of Diamond-grade vs. High-intensity Retroreflective Sheeting on Work Zone Drums

Stephen G. Busam
Graduate Research Assistant, Department of Civil Engineering, Ohio University

PROJECT SUMMARY

Each year more than 700 fatalities occur nationally due to vehicular accidents within work zones. New developments and technologies have paved the way for the creation of diamond-grade sheeting, a new, more retroreflective sheeting. Research has shown that diamond-grade sheeting is 6 to 14 times brighter then engineering-grade sheeting and is already widely required for use on work zone signs. However, the diamond-grade sheeting is not widely required for use on channelizing drums due to the increased cost and concern that the increased retroreflectivity of the sheeting may actually decrease the safety of the work zone when used on closely spaced construction drums. A comparative parallel study was conducted to compare the safety impacts of the diamond-grade sheeting with high-intensity sheeting, the current MUTCD standard. Driver behavior within the work zone was analyzed in terms of lane placement and traveled speed with respect to the posted speed limit. These data were collected and analyzed to determine the extent to which the behaviors differed between the two traffic control treatments. A current state of practices survey was also distributed to each state department of transportation to determine the extent to which diamond-grade sheeting is being used. Approximately 66.7 percent of the state departments of transportation who responded to the survey do not require diamond-grade sheeting for use in construction zones citing material cost as their reasoning. Those states that do require diamond-grade sheeting for use on drums in their work zones listed safety, improved work zone delineation, and improved work zone visibility as outweighing the cost of the sheeting. Based on the lane placement and speed deviation data, drivers traveling through work zones with diamond-grade sheeting position their vehicle further away from the work zone and abide closer to the posted speed limits when compared to those traveling through work zones with high-intensity sheeting on the construction drums.

Coupled Thermo-hydro-mechanical Model for Pavement Under Frost Action

Zhen Liu
Graduate Student, Case Western Reserve University

A multiphysical model is developed to analyze the coupled hydro-thermo-mechanical fields for porous materials to allow for the behavior of base and subgrade suffering from inclement climate. It integrates the Fourier's laws for heat transfer, Richard's equation for fluid transfer, and linear constitutive relationship. In addition to basic couplings based on thermodynamics, various coupled parameters were utilized for transferring information between field variables. Additional relationships, such as the similarity between drying and freezing processes and Clapeyron equation for ice balance were incorporated to take into account the effects of frost action. Numerical simulations were implemented in multiphysical platform to solve the coupled nonlinear partial differential equation system with typical boundary conditions. The high nonlinear problem was turned out to be solved smoothly with stable solutions which cement our understanding of the phenomena. For application, reasonable simplifications were made specifically to facilitate the problem solving process, which in return yield results lending supports quantitatively to implementation of the theoretical model. Case study on the pavement proves the practical potential of the method and verifies the validation of the model as all input base on measured data.

A brief introduction is presented for the multiphysics model for which more details can be found in [4]. Thermal field due to energy transfer is usually the main cause of the multiphysical processes. This physical field is described by a modified Fourier's equation.

$$C_{\mathrm{a}} \frac{\partial T}{\partial t} = \nabla \cdot \left(\lambda \nabla T \right) - C_{\mathrm{w}} \nabla \left(\mathbf{J} T \right) \qquad (1)$$

where C_{w} is heat capacity of unfrozen water, C_{a} is the apparent heat capacity and λ is thermal conductivity, T is the temperature, t is time and $\mathbf{J}$ is the water flux from hydraulic field. Both C_{a} and λ are coupling variables.

For variably unsaturated porous media, the fluid movement is described by a mix-type Richards' equation.

$$\frac{\partial \theta_{\mathrm{w}}}{\partial t}+\frac{\rho_{\mathrm{i}}}{\rho_{\mathrm{w}}}\frac{\partial \theta_{\mathrm{i}}}{\partial t}=\nabla\cdot\left(K_{\mathrm{Lh}}\nabla h+K_{\mathrm{Lh}}\mathbf{i}+K_{\mathrm{LT}}\nabla T\right) \qquad (2)$$

where θ_{w} is the volumetric content of water, θ_{i} is the volumetric content of ice, ρ_{w} is the density of water, ρ_{i} is the density of ice, K_{Lh} is the hydraulic conductivity, K_{LT} is the hydraulic conductivity due to thermal gradient, and $\mathbf{i}$ is the unit vector along the direction of gravity.

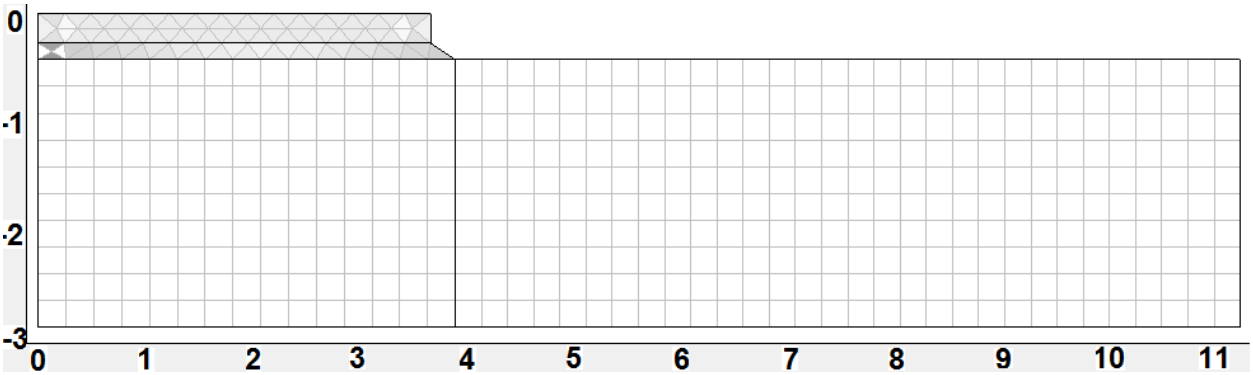

Figure 1 Meshed computational domain and boundary

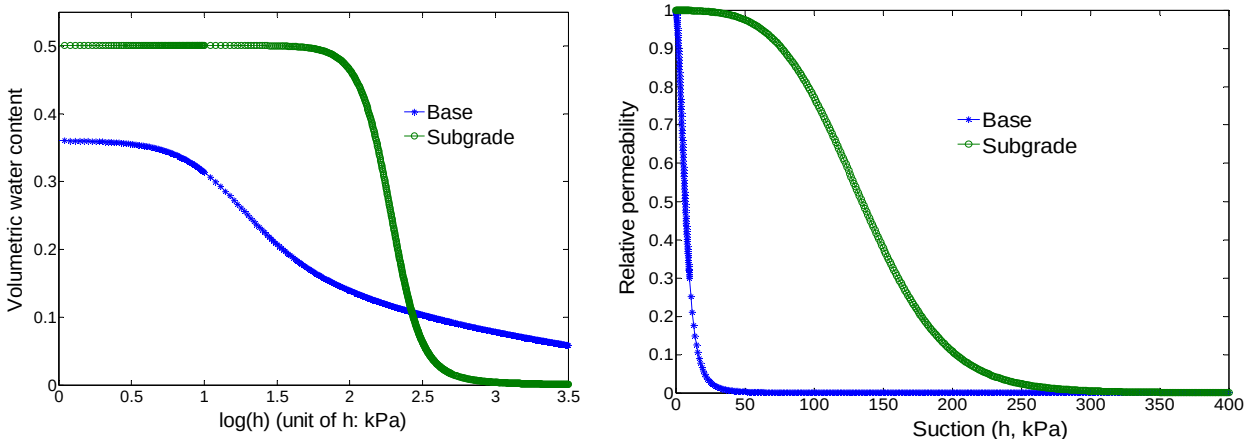

Figure 2 a) Soil water characteristic curve; b) Hydraulic conductivity versus suction

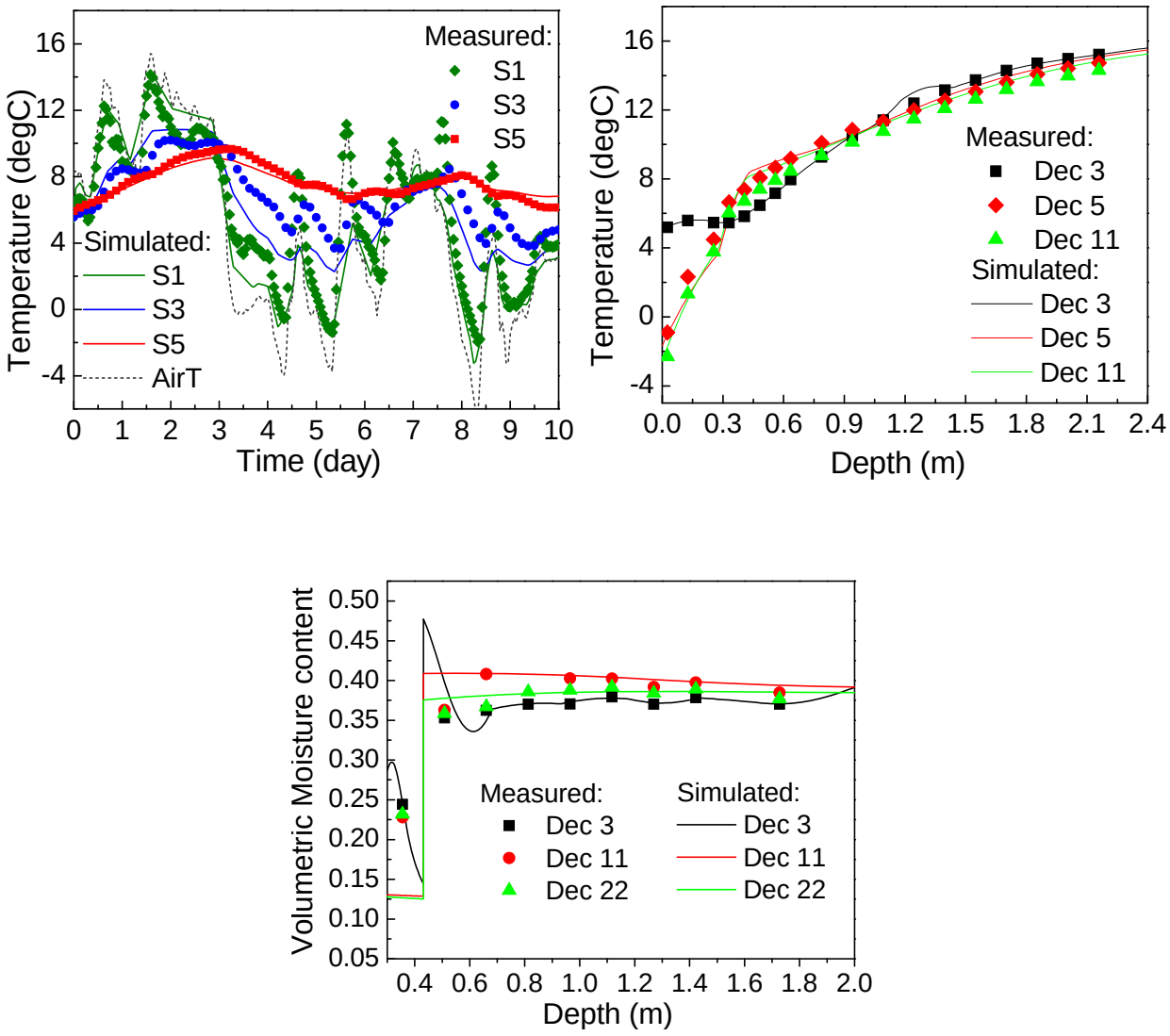

Figure 3 a) Temperature verse time; b) Temperature at different depths; c) Moisture distribution

UT Solar Car Project

Sean Sheppard, Ethan Matthews, Zachary Linkous, Sherry Ackerman
Undergraduate Students, University of Toledo

The University of Toledo Solar Car Team (UTSC) was founded in 2008 with the goal to build and race a solar-powered car in the 2012 American Solar Challenge. The event is a cross-country time/ endurance race across public highways. The team is currently designing the university's first solar car with the mission to educate students and the greater community on alternative energy and its applications, as well as to build a practical solar car that could have real world applications upon further technological advances. The team has a strong desire to innovate and use local technology and resources. Since Toledo is moving to redefine itself as America's Solar City, the UTSCT desires to build a car that stands out and represents the alternative energy community in Northwest Ohio. The team is currently designing its car and actively seeking sponsors. The final product is going to feature new and original technology including a custom built energy efficient Hub Motor as well as other unique energy-saving technologies. The organization is very excited to be part of the alternative energy solution and to help raise community awareness about solar technology.

The University of Toledo Solar Car Team (UTSC) was originally founded in 2008 but due to most of the team graduating, did not get off the ground until the summer of 2010. With momentum building, the team has chosen to focus its efforts on five main goals:

Education

Innovation

Promoting local technology

Design, build and race a *practical* solar car

Compete in the 2012 American Solar Car Challenge

We strive to educate students and the local community about various alternative energy technologies. The innovation refers to taking those previously developed technologies and trying to use them in different applications. We also aim to not only promote our University but also to help Toledo with its goal of trying to reinvent itself as the Solar City.

As for *practicality,* one way we wish to be practical is economically. We are estimating the price of our car to be somewhere between $60,000- $80,000 whereas other solar cars could be anywhere between $1 million and $10 million. We plan to keep expenses down partially by building our own motor and not using space grade solar cells. The other ways we will keep our expenses down are by the different technologies that we are planning on incorporating into our car which will maximize the car's energy usage.

Once every two years, Universities all over the country have competed in this "rayce" (the American Solar Challenge) to see who can finish first in this cross-country event ranging anywhere between 1200-1600 miles across public highways. The previous race went from Broken Arrow, OK to Naperville, IL. The next race will occur in the summer of 2012 but the specifics have not yet been announced.

Because the group was recently founded and has no previous models, the team has chosen to investigate all facets of the car to try and gain an advantage against the more established teams. Some of the mechanical aspects that the team is trying to be innovative with include: an in-wheel hub motor design, possibly airless tires, and also the body design of the car. Most cars in the Solar Car Challenge look very similar to flat pancakes on wheels. Our body design looks more like a tear drop or wing shape to increase aerodynamics and so the car resembles more of a "normal" car shape. All other mechanical aspects of the car will be consist of parts that can either be easily be fabricated or bought so as to minimize the complexity of not only building, but also working on the car.

For the upcoming race, the team has chosen to spend a lot of time innovating the electrical side of the car, trying to make it as unique as possible. This past semester, the electrical team has been busy at work researching and doing simulations to figure out the optimum design for the in-wheel hub motor design. The other electrical aspects of the car that students have been working with are the battery management system and a solar golf cart project. This battery management system uses a pulse controller, which will maximize the efficiency of energy transfer during charging and discharging of the batteries.

Another process of electrical designing is the hub motor. It is based on the unique technology invented by Flynn Motor Technologies, but our system has the unique ability to recover inductive energy while the motor is in operation, and this is in addition to the standard regenerative breaking technology. These technologies will integrated to give our car both performance, and energy efficiency advantages.

Since our car and the technology involved is a reflection of the innovations taking place at UT, we are working on various innovative electronics and battery systems to allow us to leverage some of these amorphous solar technologies in our system design to show how a solar car could someday be developed into a practical technology for everyday use.

For further information please contact:

James Price
University of Toledo Solar Car Team President
University of Toledo
2801 W. Bancroft , MS 310
Toledo , OH 43606
(419) 701-4404

utoledosolarcar@gmail.com
Priceja6@gmail.com

An Innovative Method for Soil Water Characteristic Curve Measurement with a Thermo-TDR Sensor

Zhen Liu
Graduate Student, Case Western Reserve University

The soil water characteristic curve (SWCC) characterizes the moisture retention properties of soils and responsible for important phenomena of fluid transfer, salt and ion transportation as well as mechanical deformation and failures in unsaturated soils. In this paper, a new method is proposed for SWCC measurement based on the similarity of freezing and drying processes in soils. The theoretical basis for this method is reviewed, from which the experimental procedures were developed. Matric suction and the degree of saturation (water content) is related to the temperature at equilibrium for ordinary soil and freezing/thawing soils and degree of freeze/thaw based on the similarity between the desorption/sorption (drying/wetting) process and freezing/thawing process. A thermo-TDR (time domain reflectometry) sensor which combines both temperature and conventional TDR sensors is used for synchronous measurement of the temperature and degree of freezing/thawing. The TDR function measures the free water content during the freezing/thawing processes, while the built-in thermocouples measures the internal temperature distribution. Experiments were conducted to evaluate the ability of thermo-TDR to get a complete soil freezing characteristic curve (SFC) for general porous medium. Experiment is conducted to test the performance the method of estimating the SWCC

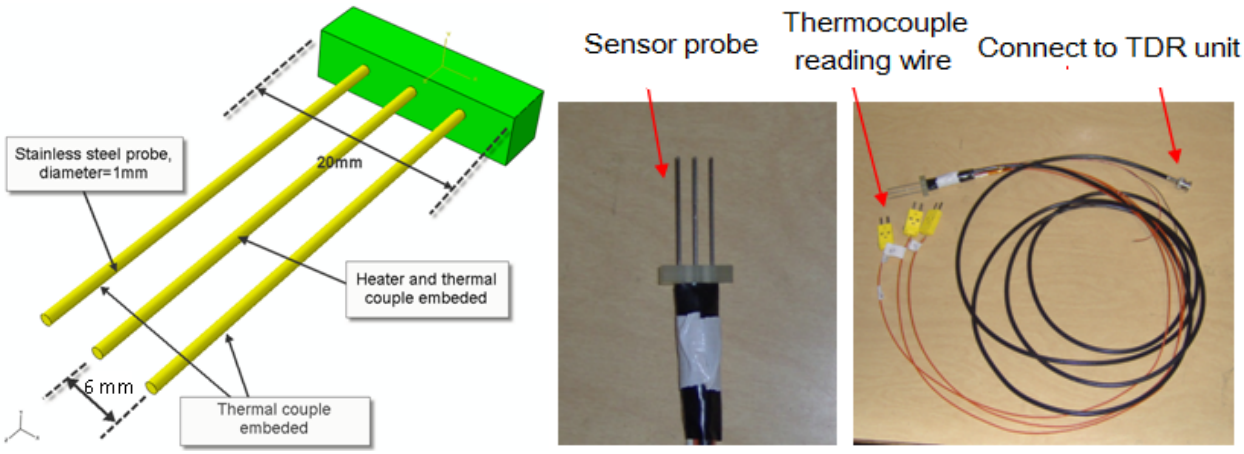

Figure 1 a) Schematic design of the thermal-TDR probe b) Photos of the fabricated thermo-TDR probe

from SFC. The results compared well with the SWCC measured by standard filer paper method. The effects of rate of thawing on SWCC estimation were investigated.

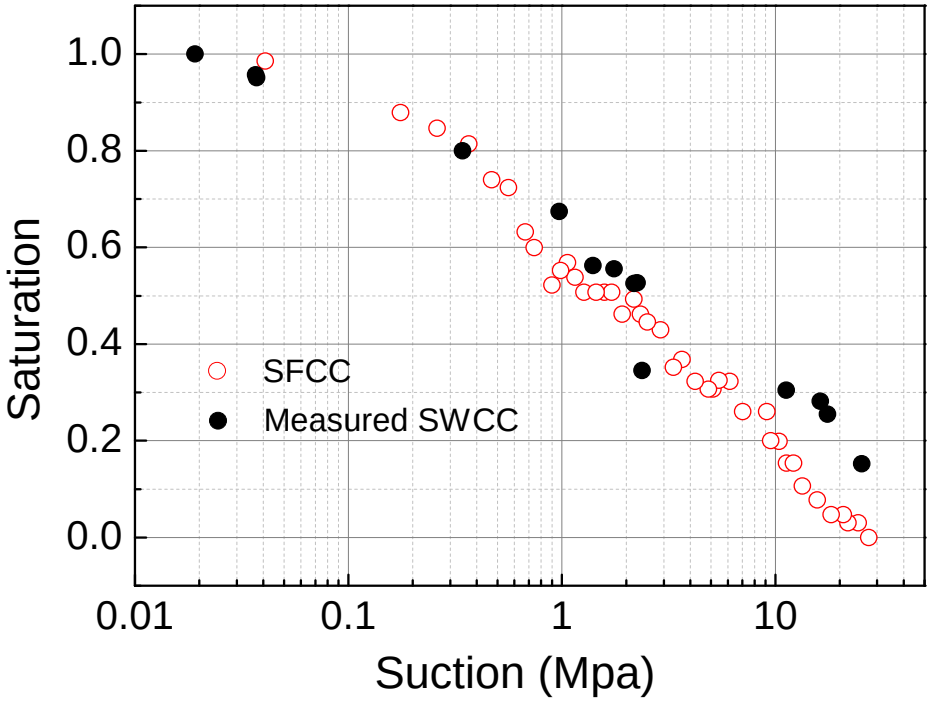

Figure 2 Measured SWCC and SFCC for a soil

Laboratory Experiments on the Variation of Hydraulic Roughness in Partially Filled Culverts for Fish Passage Design

Jay Prakash Devkota
Graduate Student, Youngstown State University

Introduction

Culverts are hydraulic conduits that serve to convey water from one side of a highway to the other. Culverts are generally a single run of pipe or box section that is open at both ends. In general, culverts serve two main purposes, first and narrowest scope is that they provide a conveyance for surface water and storm water under a roadbed or railroad grade, and secondly they allow fish and wildlife passage under the transportation route

Previously Transportation was considered only for connecting people. But with the increasing knowledge of negative effects in aquatic ecology, Engineers are now requested to design culverts that minimize the barriers for fish passage. The more common culvert materials used in the state of Ohio are HDPE and steel (smooth and corrugated).

All of the fish passage design methods seek to allow passage when fish are believed to be moving in the natural stream system. Excessive inlet velocity and inadequate water depth may restrict successful passage of fish through the culvert.

Water velocity within a culvert is a function of cross sectional area, slope, roughness and the design discharge. Among all factors, culvert roughness is the most readily manipulated factor that influences velocity. If the velocity in a culvert exceeds a certain level, it may act as a barrier to fish attempting to ascend upstream. Flow velocities can be reduced by increasing culvert size, roughness, burial depth, and by reducing culvert slope. Reduced velocities in the hydraulic boundary layer on the edge of the culvert barrels are seldom adequate for upstream fish passage through the length of the culvert.

Goal of my proposed Research

- The results of this project are expected to allow engineers to better evaluate existing culverts and to better design future culverts for fish passage.

Literature Review

My project builds on a literature review of Steve Mangin's thesis on "Reducing the Error Associated with Manning's Roughness in Culvert Design for Improved Fish Passage". He found that

velocities in culvert barrels will usually be greater at the medium flow condition than at low flow i.e. roughness is partial filled pipe/culvert is usually higher than full flow condition.

Based on the research questions that emerged as a result of Mangin's study I will be investigating data at depths below 20%.

Methodology:

The major hydraulic criteria influencing fish passage are: flow rates during migration periods: and material roughness, depth, diameter and slope of the culvert. So the data collection consists of measurement of discharge and depth for different values of diameter and slope with two different material types.

Manning's Equation:

Manning's Equation is an empirical equation applied to uniform flow in open channels.

$V = C_n/n * R^{2/3} * S^{1/2}$

Laboratory set up:

The laboratory model will be a flume of 4ft * 2ft * 60ft (w*h*l) with culvert. The culverts will be in this flume.

Fig: Laboratory set up of Flume and Pump

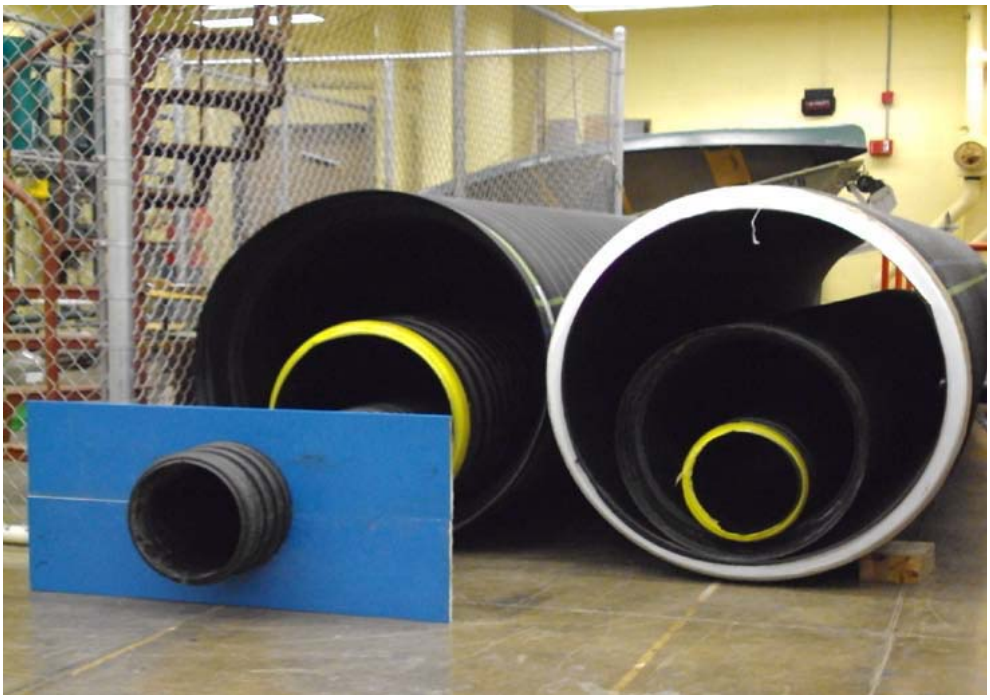

Fig: Laboratory set up of Flume and Pump

Once the culvert is placed inside the flume and with the help of a pump the water is pumped into the flume at a rate of up to 12 cuft/sec. The pump has overall 38 turns. The flume has a tilting bed so that we can change the slope of the flume/ culvert by adjusting from the bed of the flume.

Work Status:

Accomplished work:

- The week before I arrived, the flume was not functional.
- At this point the flume is one step away from being usable for culvert tests.
- Preparation for setup of the flume and making supports for the culverts.
- Up to 38 turns of the valve have been completed for the discharge rating curve.

Remaining work:

- Putting the culverts in the flume. This will be done by the pulley system hanged in the ceiling of the lab.
- Making provisions for depth measurement in the culvert by making hole or by drilling.

➢ Finally depth measurement for each of the different values of discharge, diameter, slope and material will be done.

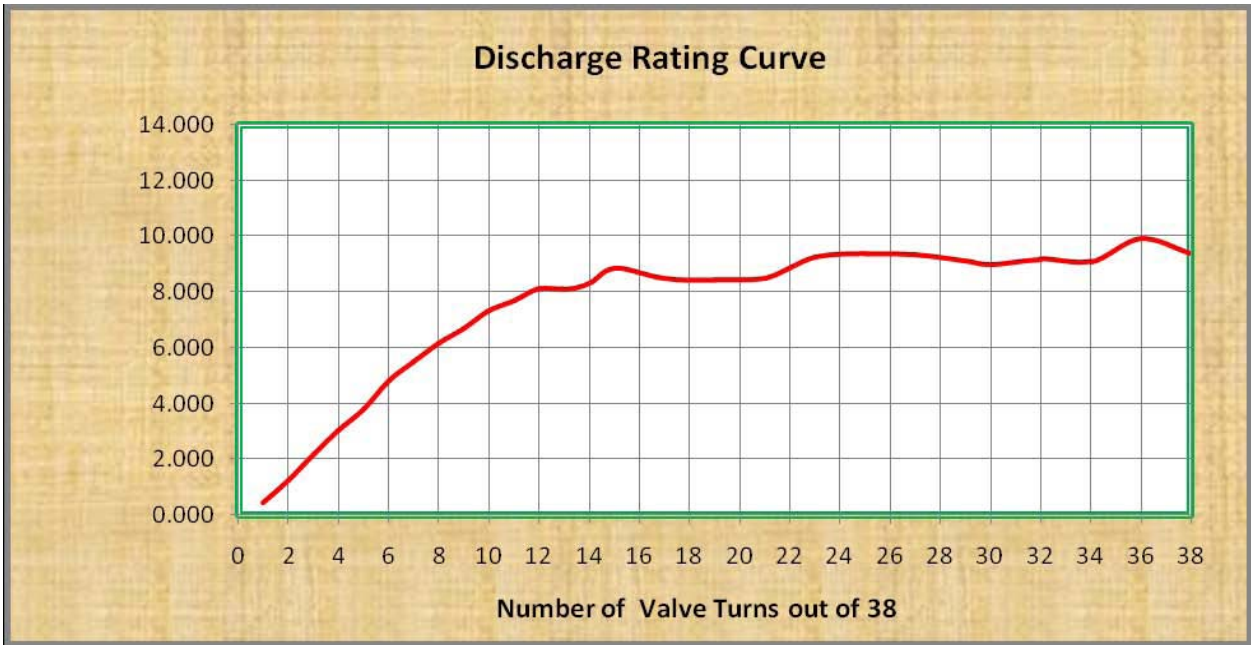

Fig 1: Discharge Rating Curve

Conclusion:

By the end of this project I planned to come up with an equation that relates Manning's roughness coefficient with flow depth in partially filled culverts. As a result I expect that the relation generated will allow engineers to better evaluate existing culverts and to better design future culverts for fish passage.

Estimating On-Road Mobile Source Pollution in Ohio

Ramanitharan Kandiah
Assistant Professor, International Center for Water Resources Management, Central State University

André Morton and John Davenport
Undergraduate Students, International Center for Water Resources Management, Central State University

Introduction

Air pollution is significantly related to number of health, environmental and also economical effects. Controlling and mitigating air pollution starts with the understanding of the pollutants, their sources, and the dispersion mechanisms. Mobile sources that significantly contribute the pollutants to the air can be sub-classified into two groups; On-Road Mobile Sources (ORMS) and Nonroad mobile sources. ORMS which are the concern of this paper are comprised of the vehicles used for transportation on roads. This category includes light-duty vehicles, light-duty trucks, heavy-duty vehicles, and motorcycles. They are mostly operated by variety of fuels, mainly gasoline and diesel, and to a little extent by natural gas, ethanol and electricity. The On-Road Mobile Source Pollutants (ORMSP) that are emitted from the ORMS include Hydrocarbons, Carbon Monoxide (CO), nitrogen oxides (NO_x), particulate matter (PM), air toxics and greenhouse gases. Emitted quantity from an on-road vehicle depends on various factors; type of the vehicle, age and operating condition of the vehicle, type of the powering fuel, speed the vehicle runs and the distance it travels. Further, the total quantity of ORMSAP present in the atmosphere depends on the number of vehicle travels, the time of the day and the surrounding environment too. Given the number of the players involving in the pollution mechanism, it is difficult to get an accurate estimate for the ORMSAP in the atmosphere.

This paper presents a methodology that provides preliminary estimates for the ORMSPs released in each counties of a region. The methodology is demonstrated with a case study in the counties of Ohio.

Methodology

Total Emission for Segment (TES) is defined as the metrics of all individual ORMSP emissions for a road segment. It is computed as the product of Vehicle Miles Traveled (VMT) and actual emissions of ORMSPs per mile. Total emission of each ORMSP in the interested area (such as a county) is computed

by adding the TES metric of the particular ORMSP within that area. The emission intensity, defined as emitted ORMSP quantity per area is calculated by dividing the total emission by the area. The findings are visualized on ArcGIS.

Case Study

Annual Average Daily Traffic (AADT) count data for cars and trucks for three types of routes (state route, US route and interstate route) for six year period (2003-2007) in Ohio was obtained from ODOT. CO, PM and NO_x emissions per mile were assumed as those of the allowable emissions provided in Tier 2 standard (Diesel Net, 2010). Figure 1 shows the Ohio highways system.

Figure 1: Ohio Highway Network

Results, Discussion and Conclusion

Figures 2, 3 and 4 show the Ohio counties with respect to the total particulate matter, NOx and CO emissions in the counties. Cuyahoga County, Franklin County and Hamilton County were found to have the highest level of emissions for these three pollutants. Considering the traffic in the metropolitan cities in Cuyahoga County (Cleveland), Franklin County (Columbus) and Hamilton County (Cincinnati) the high levels of emissions are expected. Rural counties with less traffic -especially those counties that do not have any interstate highway passing through them - received the lowest quantities. Among the two types of vehicles we studied, passenger vehicles were found to contribute a

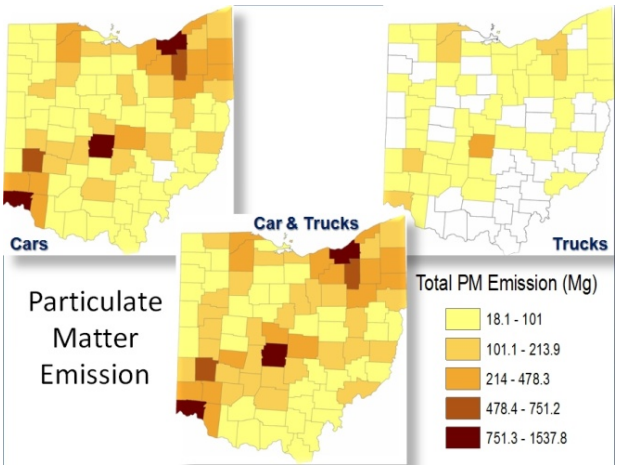

Fig 2: Ohio Counties according to PM Emission Levels

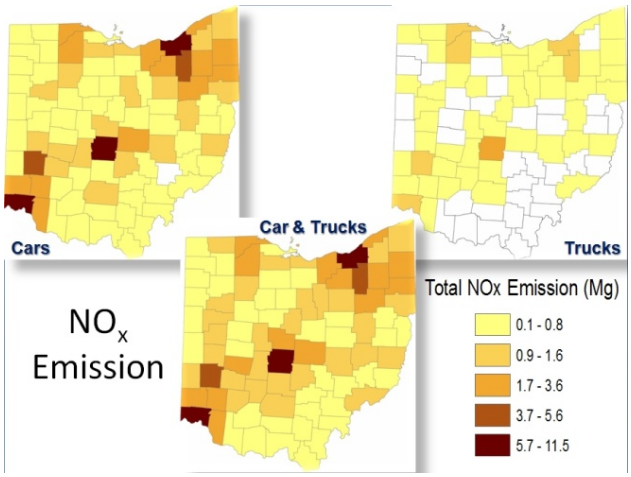

Fig 3: Ohio Counties according to NOx Emission Level

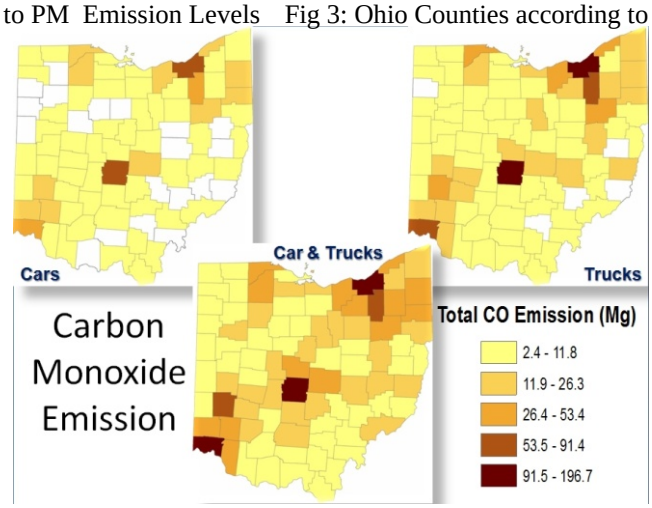

Figure 4: Ohio Counties according to CO Emission Level

larger portion in to the pollution, though a truck (heavy duty vehicle) emits more than a car (light duty vehicle) emits. This approach can be improved by incorporating better individual pollutant emission estimates for a vehicle using programs like MOVES (EPA, 2010).

Acknowledgement

The authors thank the Ohio Transportation Consortium for financially supporting this study.

We also want to thank Ohio Department of Transportation for providing the data.

References

Diesel Net Homepage: *Cars and Light-Duty Trucks—Tier 2*; See http://www.dieselnet.com/ standards/us/ld_t2.php (accessed September 2010)

USEPA; *MOVES (Motion Vehicle emission Simulator).* U.S. Environmental Protection Agency; See http://www.epa.gov/otaq/models/moves/index.htm (accessed September 2010)

Traffic Data Collection Using Multi-Touch Technology on Mobile Device

Yunke Du and Yikun Wang
Graduate Students, Department of Civil Engineering, The University of Akron

Conventional methods of traffic data collection are labor-intensive and time-consuming. Manually transcribing traffic data and entering into a spreadsheet is not only ineffective but also error-prone. Automatic traffic data collection by detectors and other traffic sensors requires installation of expensive hardware equipment costly to maintain, yet some critical information, such as vehicle turning movements and intersection delay, is hard to obtain due to lack of vehicle tracking capability by the detectors/sensors and the limitations of data processing algorithms.

As an improvement, we developed a multi-touch technology based data collection system that includes two modules:

Vehicle Turning Movements Module

Vehicle Turning Movements Module is based on pattern recognition over input gestures to identify Vehicle Turning Movements.

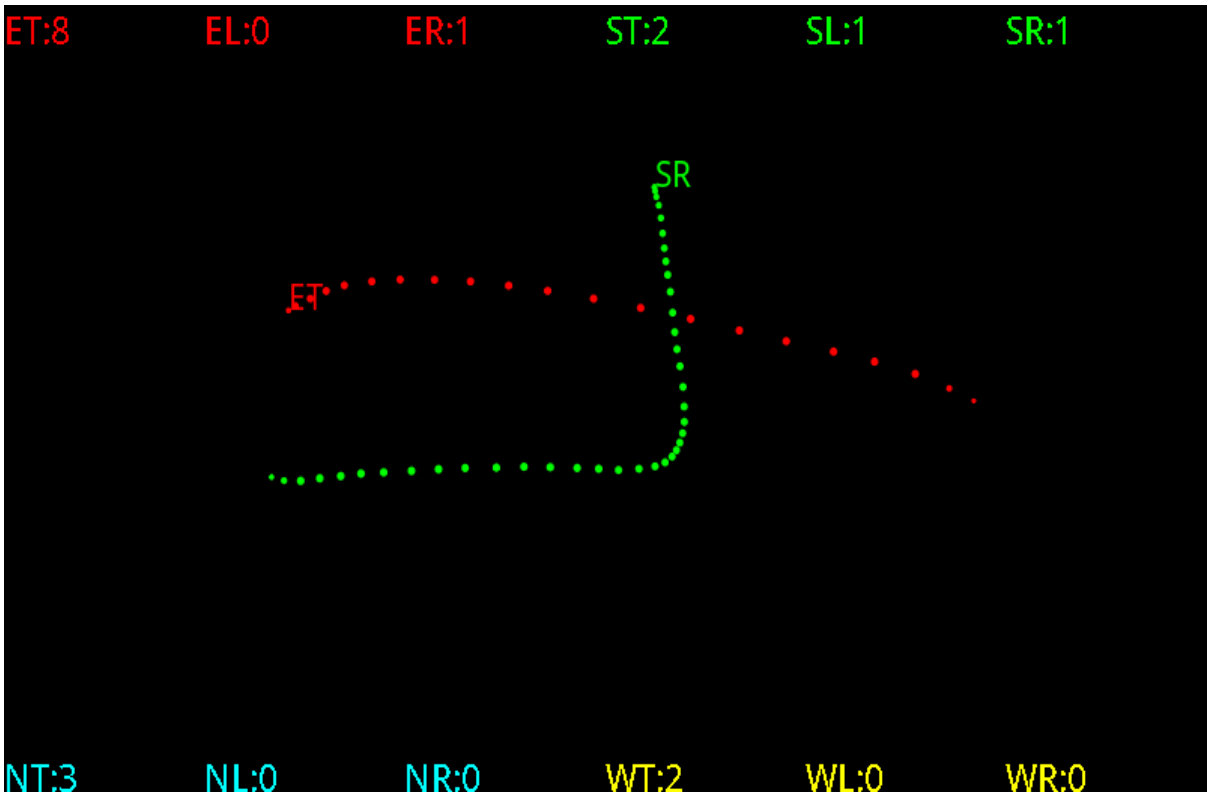

Intersection Delay Measurement Module

Intersection Delay is calculated by actual travel time subtracts free flow travel time. In order to obtain actual travel time, the system records the time when a vehicle passes a preset reference point and when the vehicle leaves the intersection. Free flow travel time can be calculated by inputting travel length and free flow speed.

The system uses a smartphone with Android operating system which is based upon a modified version of Linux kernel to take advantage of multi-touch technology for movement identification and object tracking. The algorithms are written in Java. Preliminary tests of the two above modules have been conducted; the results of this study has demonstrated the feasibility of the proposed method and its future promise.

Effects of Left-Side Ramps on Crash Frequency on Urban Freeway Segments

Aline R. Aylo and Worku Y. Mergia
Graduate Students, University of Dayton

The purpose of this study is to explore the effects of factors which can be categorized into geometric design elements, human/driver related factors, traffic and environmental factors on a on a 6.5 mile section I-75 that passes through downtown Dayton. This section encompasses about 46 ramps between Edwin C Moses Boulevard and Needmore Road interchanges. Police reported crash data retrieved from Ohio Department of Public Safety (ODPS) crash database for the years 2005 through 2008 was used. Crashes associated with merging and diverging ramps were screened using the HCM definition for merge and diverge influence area as shown in Figure 1. Two datasets were prepared one for merging ramp influence areas and a second for diverging ramp influence areas. Table 1 (next page) shows a statistical summary and the list of independent variables and the dependent variable in the model.

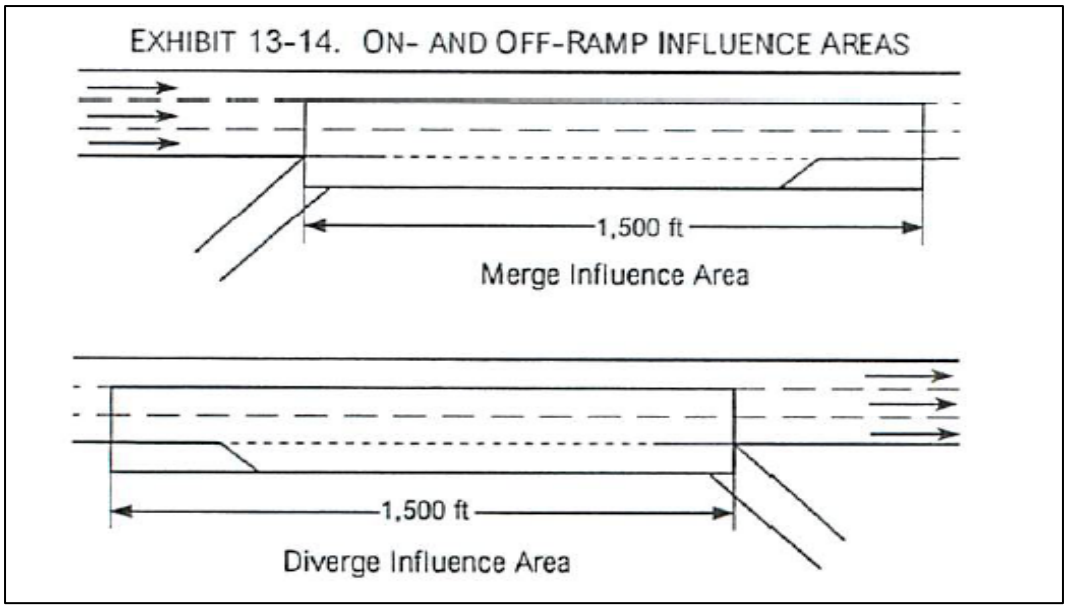

Figure 1

Over-dispersion in the data was checked to select the appropriate statistical distribution that can be applied to build the model. The first test of over-dispersion which compares the variances and means showed that the variances are significantly larger than the means for both datasets. The quotients of the Pearson's chi-square statistic and the degree of freedoms also are greater than one

Table 1 Summary of the variables considered for the merging data

Variable	Description		Variable type	Frequency merging	Frequency diverging
VC	Annual average daily traffic	in 1000's of vehicles	Continuous	721	804
W	Weather	1-adverse	Class	202	172
		2-normal		519	632
LTC	Light Condition	1-adverse	Class	191	172
		2-normal		530	632
RC	Road Condition	1-adverse	Class	237	213
		2-normal		484	591
Age	Age of the driver	1-under 21	Class	132	142
		2-over 65		39	51
		3- btw 21 & 65		550	611
WZ	Work Zone	1-work zone	Class	88	112
		2-not a work zone		633	692
BD	Bridge	1-bridge	Class	459	529
		2-not a bridge		262	275
MR	Merging	1-merging left	Class	58	--
		2-merging right		663	--
DV	Diverging	1-diverging left	Class	--	220
		2-diverging right		--	584
Total				**721**	**804**

and the p-values of the variables are less than one. The 95% confidence intervals of k are [0.0730, 0.2928] for merging and [0.1427, 0.3977] for diverging. The intervals do not contain zero. In addition the p-values of Lagrange multiplier test are less than 0.0001, indicating that the data are over-dispersed making the negative binomial distribution an appropriate distribution.

Table 2 Negative binomial generalized linear model estimation results for merging

Variable	Estimated coefficient	Std. Error	Wald 95% Confidence Limits		Wald Chi-Square	Pr > ChiSq
Intercept	-5.8977	0.6425	-7.1569	-4.6385	84.27	<0.0001
MR	2.0644	0.1855	1.7008	2.4280	123.85	<0.0001
RC	0.6119	0.1409	0.3358	0.8881	18.87	<0.0001
LTC	0.7804	0.1451	0.4959	1.0649	28.91	<0.0001
WZ	1.3703	0.1794	1.0187	1.7219	58.34	<0.0001
AGE 1	-1.1679	0.1625	-1.4864	-0.8494	51.65	<0.0001
AGE 2	-2.0804	0.2253	-2.5220	-1.6389	85.27	<0.0001
Dispersion	0.1829	0.0561	0.0730	0.2928		

Table 3 Negative binomial generalized linear model estimation results for diverging

Variable	Estimated coefficient	Std. Error	Wald 95% Confidence Limits		Wald Chi-Square	Pr > ChiSq
Intercept	-3.6663	0.5575	-4.7590	-2.5736	43.25	<0.0001
DV	0.8143	0.1476	0.5249	1.1036	30.42	<0.0001
RC	0.8579	0.1457	0.5724	1.1434	34.69	<0.0001
LTC	0.9905	0.1521	0.6924	1.2886	42.42	<0.0001
WZ	1.0022	0.1751	0.6590	1.3455	32.76	<0.0001
AGE 1	-1.1329	0.1639	-1.4542	-0.8116	47.76	<0.0001
AGE 2	-1.6840	0.2181	-2.1114	-1.2565	59.62	<0.0001
Dispersion	0.2702	0.0651	0.1427	0.3977		

The GENMOD procedure in SAS (version 9.3) using the negative binomial distribution was used for the development the models. Tables 2 and 3 show the negative binomial generalized linear estimation results and the corresponding p-value statistic for the merging and diverging models respectively.

Finally, the two models can be written as shown in the following two equations.

$$P_{off\ -\ ramps} = e^{-3.6663} \times e^{0.8143 DV} \times e^{0.8579 RC} \times e^{0.9905 LTC} \times e^{1.0022 WZ} \times e^{-1.1329 AGE1} e^{-1.6840 AGE2}$$

$$P_{on\ -\ ramps} = e^{-5.8977} \times e^{2.0644 MR} \times e^{0.6119 RC} \times e^{0.7804 LTC} \times e^{1.3703 WZ} \times e^{-1.1679 AGE1} e^{-2.0804 AGE2}$$

Where: P is the expected total number of crashes, MR is the merging left indicator (=1 to merging left; 0=otherwise), DV is the diverging left indicator (=1 to diverging left; 0=otherwise), RC is the road condition indicator (=1 to adverse road condition; 0=otherwise), LTC is the light condition indicator (=1 to adverse light condition; 0=otherwise), WZ is the work zone indicator (=1 to work zone; 0=otherwise), AGE1 is the age under 21 indicator (=1 to age under 21; 0=otherwise), AGE2 is the age over 65 indicator (=1 to age over 65; 0=otherwise).

The results from these models can be explained as:

- In merge areas about 7.87 times more crashes are expected to occur near ramps *merging on the left* side compared to ramps merging on the right. Similarly, about 2.25 times more crashes are expected to occur near ramps *diverging on the left* compared to ramps diverging on the right.

- Expected count of crashes due to *adverse roadway conditions such as wet pavement, snow and ice* are found to be 1.84 times more near merging ramps and about 2.36 times more near diverging ramps.
- The expected crash counts due to *adverse light conditions* such as darkness and glare are found to be 2.18 times more compared to normal daylight conditions near merging ramps and 2.70 times more near diverging ramps.
- The expected count of crashes due to the presence of *construction work zone sections* are found to be 2.78 times more than sections with no construction near merging ramps and they are 3.94 times more near diverging ramps.
- The expected count of crashes near merging ramps is lesser by a factor of 0.125 for senior drivers (Age>64) and 0.313 for youth drivers (Age <21) compared to drivers of age range 21-64.
- Similarly, expected count of crashes near diverging ramps show a decrease by a factor of 0.186 for senior drivers (Age>64) and 0.322 for youth drivers (Age<21) compared to the drivers of age range 21-64.

In conclusion, the prediction model developed here can be used to evaluate the safety performance of left-side ramps. Left-side on- and off-ramps are critical traffic safety factors, therefore, future designs should avoid the provision of ramps on the left side and safety improvements should consider the safety benefit of replacing them with right-side ramps.

Evaluating Traffic Safety Behaviors of College Students

Sowjanya Ponnada
Graduate Studetn, Department of Civil and Environmental Engineering and Engineering Mechanics, University of Dayton

This paper explores the traffic safety behavior of 18-24 yr old college students who annually experience alcohol-related deaths, injuries and other health problems. In addition, college student's perceived causes related to smoking and also not following safety measures while driving and their opinions on how to reduce the accidents were included. A sample of 107 full time undergraduate civil engineering students at University of Dayton participated in the questionnaire survey that assessed their demographic characteristics, drinking-driving, precautionary measures to avoid traffic accidents, being involved in crashes as a driver and/or as being involved in crashes when riding in a vehicle driven by someone, smoking and drinking behavior. The majority of the students reported that they never drink alcohol while. In contrast, the same students reported that they had been driven by an intoxicated driver and almost one-third of the students reported that they smoke or consume alcohol. Age, gender and class, type of vehicle may play part in the evaluation of drinking - driving behavior, smoking-drinking and being involved in a crash. According to this study alcohol-related, driving-risk behaviors among college students become worse at the age of 21. There is need to investigate further the relationship between the students who consume alcohol while driving and riding with an intoxicated driver, the major reasons to involve traffic crashes.

Dynamic Dilemma Zone at Signalized Intersections: Safety Issue and Solutions

Zhixia Li
Ph.D. Candidate, Advanced Research in Transportation Engineering and Systems Laboratory
School of Advanced Structures, College of Engineering and Applied Science, University of Cincinnati

Summary:

At high speed signalized intersections, the issue of yellow light dilemma is known as a major cause of rear-end and right-angle crashes. This dilemma is typically characterized by a physical zone in advance of the intersection, which is termed as dilemma zone (DZ). Drivers in DZ at the onset of yellow indication are forced to make a stop/go decision during a very short period. And, an improper decision may lead them to a potential rear-end or right-angle crash. Therefore, it is critical to accurately estimate the exact location of DZ in order to provide necessary DZ protection to drivers. However, one apparent barrier in accurately estimating the DZ locations lies in the uncertainty of modeling dynamics of DZ. Traditional method for computing DZ uses constant contributing factor values that cannot reflect the dynamic features of DZ. This issue has been recognized for many years. In other word, quantitative study of the inherent DZ contributing factors remains a challenge. Lack of effective means for gaining the trajectory data over the yellow interval may be a key reason.

In this research, the author upgraded the software VEVID (**Ve**hicle **Vi**deo-Capture **D**ata Collector) developed by the author's advisor. The upgraded VEVID make it practical to obtain vehicle trajectory data from video, such as vehicle's distance from stop line and vehicle's speed at every 1/30 second during the yellow interval including the onset of yellow time. Significantly, this video-based approach has been proved to be an accurate and cost-effective way for extracting vehicle trajectory data through data validation process. Therefore, using this approaching, it becomes possible to reveal the dynamic features of DZ contributing factors and model the extract location of dynamic DZ. The trajectory data of 1445 vehicles are extracted in total from 46-hour high resolution videos at four high-speed signalized intersections in Ohio using VEVID. The statistical analyses of the obtained trajectory data quantitatively disclose the dynamic natures of major DZ contributing factors, such as the driver's minimum perception-reaction time (PRT), the vehicle's maximum acceleration rate, and the vehicle's maximum deceleration rate. The results indicate that (1) the minimum PRT is greatly influenced by the vehicle's speed and can be mathematically modeled as a function of the speed by the Inverse model. i.e., the minimum PRT decreases as the vehicle's speed increases (See Figure 1); (2) the maximum

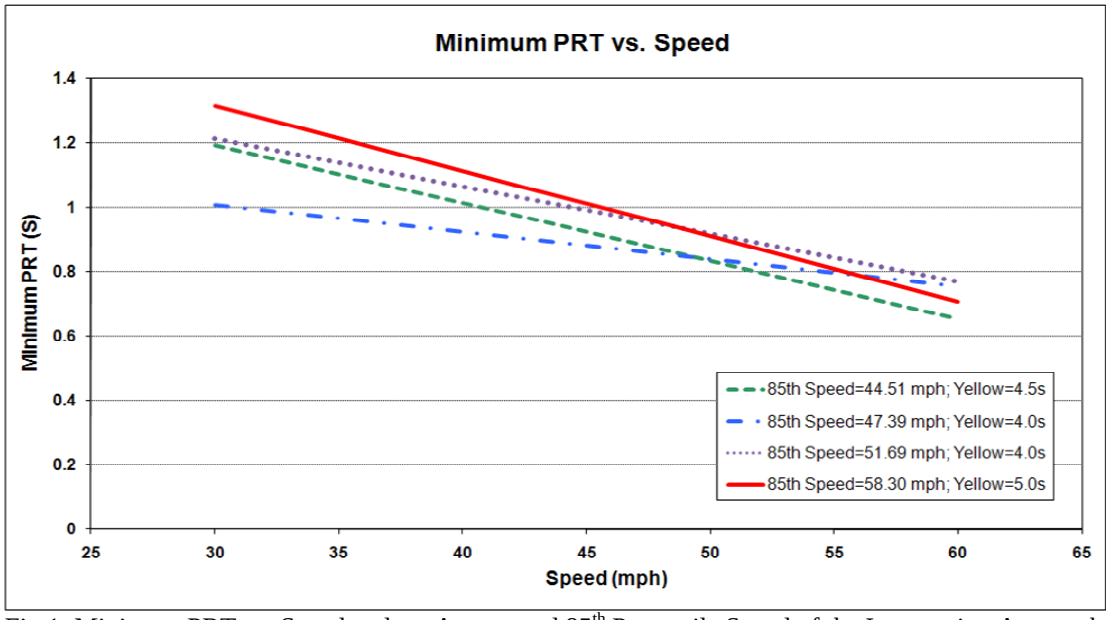

Fig 1: Minimum PRT vs. Speed and vs. Aggregated 85th Percentile Speed of the Intersection Approach

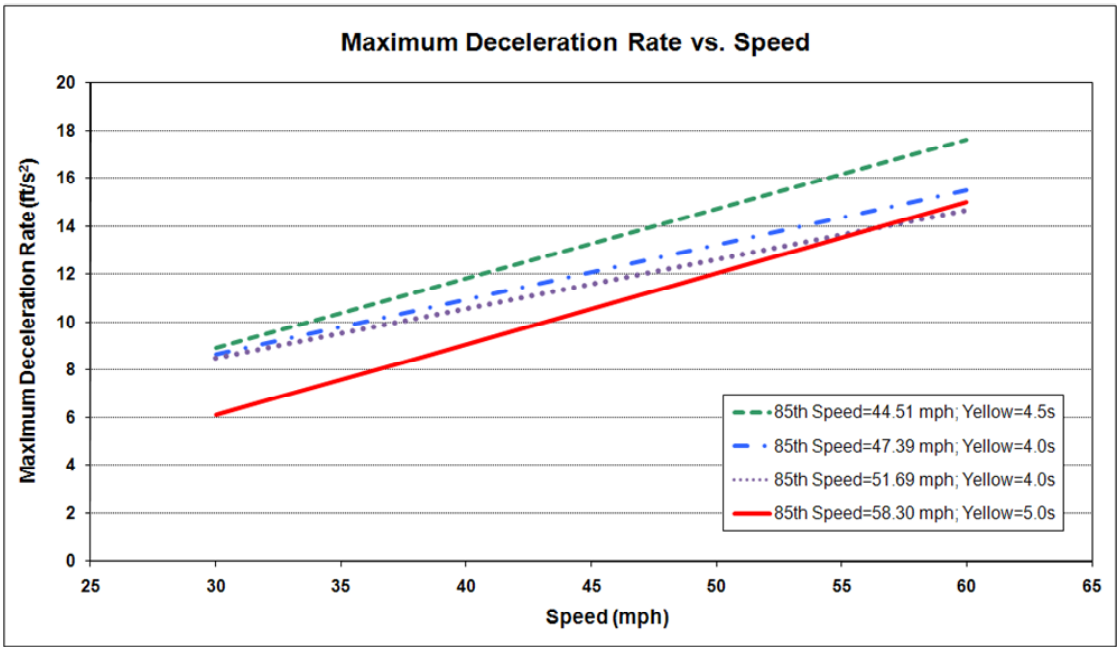

Fig 2: Maximum Deceleration Rate vs. Speed and vs. Aggregated 85th Percentile Speed of the Intersection Approach

deceleration rate and the maximum acceleration rate are greatly dependant upon both the vehicle's speed and the aggregated 85th percentile speed of the intersection approach, and can be mathematically expressed as nonlinear functions of these two variables; (3) the maximum deceleration rate increases as the vehicle's speed increases, while the maximum acceleration rate decreases as the vehicle's speed increases (See Figure 2 and Figure 3); and, (4) under the same vehicle's speed, the higher the 85th percentile speed of the intersection approach is, the smaller the maximum

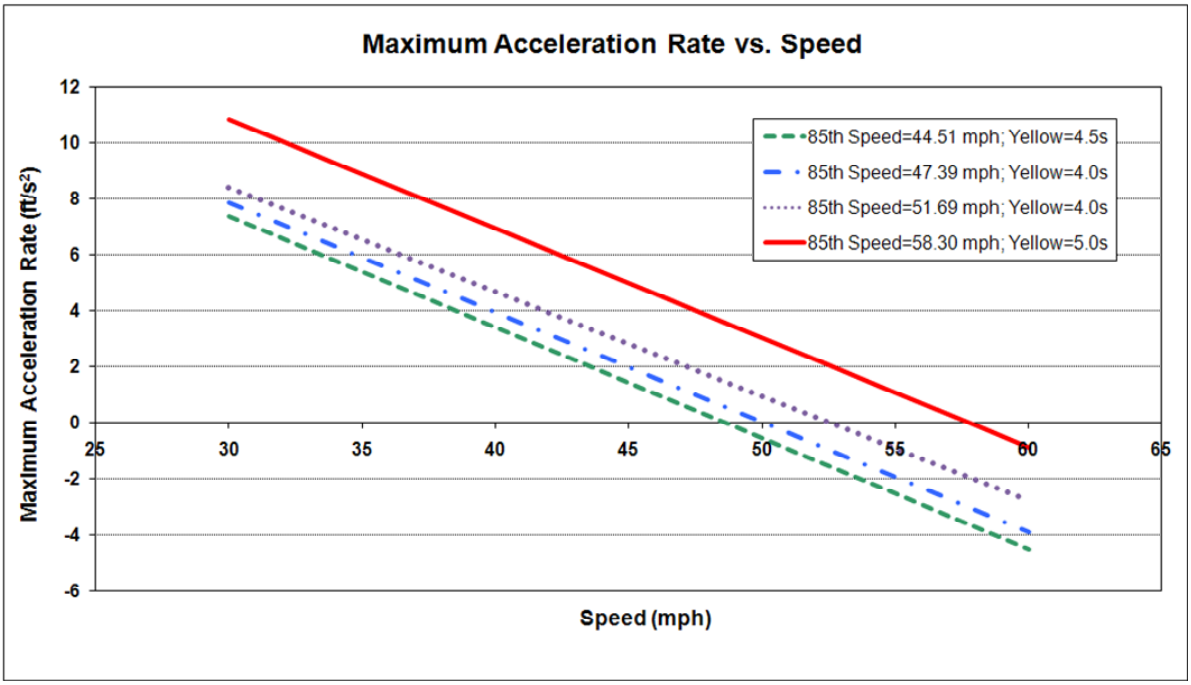

Fig 3: Maximum Acceleration Rate vs. Speed and vs. Aggregated 85th Percentile Speed of the Intersection Approach

deceleration rate and the larger the maximum acceleration rate will be (See Figure 2 and Figure 3). These results have thoroughly unveiled the uncertainty regarding the dynamics of DZ contributing factors. And, the resulted mathematical models of the contributing factors have modified and greatly improved the traditional DZ model to reflect the dynamic features of DZ. Significantly, improved DZ model is applied in updating the existing DZ table in Ohio, so that the accuracy of locations of DZ at different speeds has been greatly improved.

In order to ameliorate DZ related safety problems, advance loop detectors are typically placed at the boundaries of DZs to provide green extensions by clearing approaching vehicles out of the DZ before the onset of the yellow indication. Therefore, another objective of this research aims at evaluating ODOT's current practice of advance loops placement in terms of safety performance and operational efficiency. Moreover, an alternative layout that can enhance both safety and the operation efficiency of ODOT's current practice are also targeted in this research. During evaluation process, the operation efficiency is evaluated by the overall intersection delay, while the safety performance is evaluated by the dilemma hazard.

Traditionally, the dilemma hazard is measured by average number of vehicles in DZ for each cycle. However, previous studies have recognized that the dilemma hazard cannot be simply measured by number of vehicles in DZ, but rather comprehensively dependent on each vehicle's position and speed

at the onset of yellow time. Therefore, in the research, the dilemma conflict potential (DCP) concept is proposed to mathematically model the dilemma hazard faced by each vehicle approaching the intersection. It reflects the probability for a target vehicle to have right-angle and rear-end conflicts based on the yellow-onset speeds and locations of the target vehicle and its leading vehicle. The safety performance can therefore be measured by the number of traffic conflicts (rear-end and right angle) per hour due to the existence of dilemma zone. Before the evaluation process, The DCP model has been calibrated using the field observed trajectory data.

The evaluation results indicate that the ODOT practice reduces the dilemma zone related traffic conflicts by at least 70% at different speed limit conditions. In overall, it is more effective in providing dilemma zone protection than the scenario without advance loops (See Table 1). However, it is the current method is proved insufficient to enhance the operational efficiency of the intersection in great part. Typical evidence lies in the evaluation findings that the overall intersection delay is greatly increased at the speed limit of 55 mph if the current loop placement method is used.

Table 1: Evaluation Results of ODOT's Current Practice on Advance Loops Layout

		Speed Limit			
		40mph	45mph	50mph	55mph
Hourly DZ-Related Traffic Conflicts (Safety Performance)	No Loops (before)	3.36 conflicts/hr	2.08 conflicts/hr	1.67 conflicts/hr	1.11 conflicts/hr
	ODOT Layout (after)	0.39 conflicts/hr	0.16 conflicts/hr	0.44 conflicts/hr	0.32 conflicts/hr
	Safety Enhanced by (Conflicts reduced by)	88.39%	92.31%	73.65%	71.17%
Overall Intersection Delay (Operational Efficiency)	No Loops (before)	9.13 s/veh	9.38 s/veh	9.37 s/veh	9.19 s/veh
	ODOT Layout (after)	8.76 s/veh	8.97 s/veh	9.13 s/veh	9.32 s/veh
	Operational efficiency Enhanced by (Delay reduced by)	4.06%	4.36%	2.62%	-1.44%
Max-out Occurrence Percentage	ODOT Layout	1.85%	5.66%	16.84%	22.14%

Table 2: Comparison between ODOT Layout and Proposed Alternative Layout

		Speed Limit			
		40mph	**45mph**	**50mph**	**55mph**
Hourly DZ-Related Traffic Conflicts (Safety Performance)	No Loops Baseline	3.36 conflicts/hr	2.08 conflicts/hr	1.67 conflicts/hr	1.11 conflicts/hr
	ODOT Layout (reduced by %)	0.39 conflicts/hr (88.39%)	0.16 conflicts/hr (92.31%)	0.44 conflicts/hr (73.65%)	0.32 conflicts/hr (71.17%)
	Alternative Layout (reduced by %)	0.18 conflicts/hr (94.52%)	0.09 conflicts/hr (95.56%)	0.26 conflicts/hr (84.41%)	0.12 conflicts/hr (89.55%)
Overall Intersection Delay (Operational Efficiency)	No Loops Baseline	9.13 s/veh	9.38 s/veh	9.37 s/veh	9.19 s/veh
	ODOT Layout (reduced by %)	8.76 s/veh (4.06%)	8.97 s/veh (4.36%)	9.13 s/veh (2.62%)	9.32 s/veh (-1.44%)
	Alternative Layout (reduced by %)	7.45 s/veh (18.47%)	7.72 s/veh (17.71%)	7.83 s/veh (16.49%)	8.04 s/veh (12.53%)
Max-Out Occurrence Percentage	ODOT Layout	1.85%	5.66%	16.84%	22.14%
	Alternative Layout	0.00%	0.00%	1.34%	0.28%

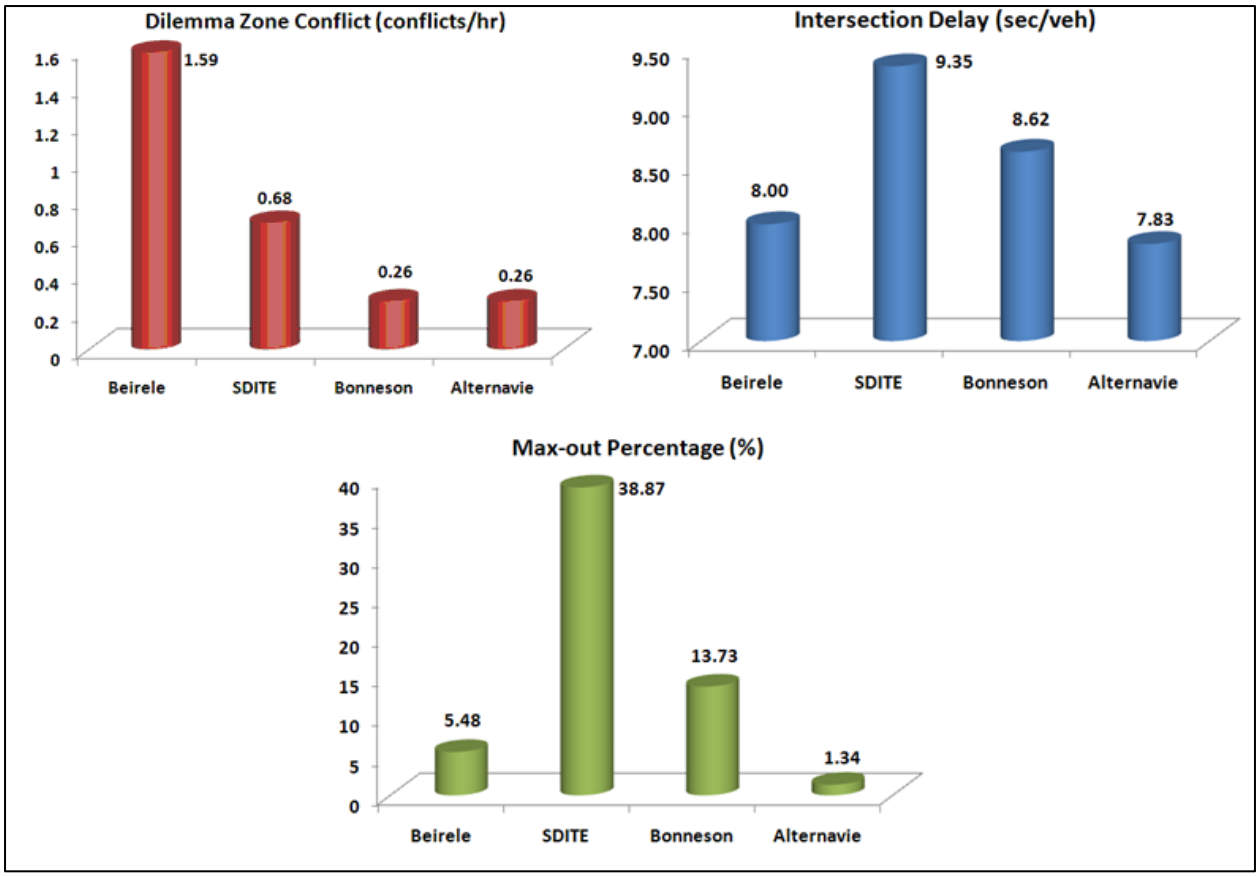

Fig 4: Comparison between Classic Layouts and Proposed Alternative Layout (50mph)

The proposed alternative loops placement outperforms the ODOT's current practice in terms of reducing the dilemma zone related traffic conflicts by at least 84% under different speed limits. Significantly, it also performs better in terms of both operational efficiency and max-out occurrence percentage at all speed limits, particularly in the case of higher speed limits such as 50 mph and 55 mph (See Table 2).

Finally, the proposed alternative loops layout is compared with other classic advance loops layouts that are widely used in the US (See Figure 4). The result has proved that the proposed alternative layout is superior to the classic Bonneson, Beirele, and SDITE layouts in terms of both safety performance and operational efficiency. Using 50 mph speed limit as an example, the comparison results indicate that the alternative layout is 6 times safer, 1.03 times more efficient, and 4 times less likely to max out as compared with the Beirele configuration. As compared with the SDITE configuration, it is 2.6 times safer, 1.2 times more efficient, and 29 times less likely to max out. The optimal layout is as safe as the Bonneson configuration, but it uses one less detector. And, it is 1.1 times more operationally efficient and 10 times less likely to max out when compared with the Bonneson configuration.

In summary and significantly, the methodology used in this research has potential to provide a theoretical base for other states in the U.S. for updating their existing DZ tables as ones that reflect the DZ dynamics, and comprehensively evaluating their existing advance loops layout strategies.

(This presented study is supported by an OTC grant and an ODOT/FHWA grant, and advised by the author's advisor, Dr. Heng Wei, Associate Professor at University of Cincinnati. Tel: (513) 556-3781; Email: heng.wei@uc.edu)

Estimating Vehicle Length under Traffic Congestion

Qingyi Ai
Ph.D. Candidate, Advanced Research in Transportation Engineering and Systems Laboratory
School of Advanced Structures, College of Engineering and Applied Science, University of Cincinnati

Accurate measurement of vehicle length provides reliable information sets for effective traffic operation and management, calibration of travel demand forecasting models, freight studies, pavement design, and even emission impact analysis of traffic operation. Dual-loop detector is one of typical sensors for monitoring freeway traffic, and it would be a potential real-time data source for length-based vehicle classifications if it held a technical promise in accuracy. However, the existing dual-loop based vehicle classification model has been only evaluated against free traffic, and higher error has been reported against congested traffic. To identify the problem so as to explore its potential in increasing the accuracy of vehicle classification, the author evaluated dual-loop length-based vehicle classification models against concurrent ground-truth video vehicle trajectory data at the selected loop stations in Columbus, Ohio (Figure 1).

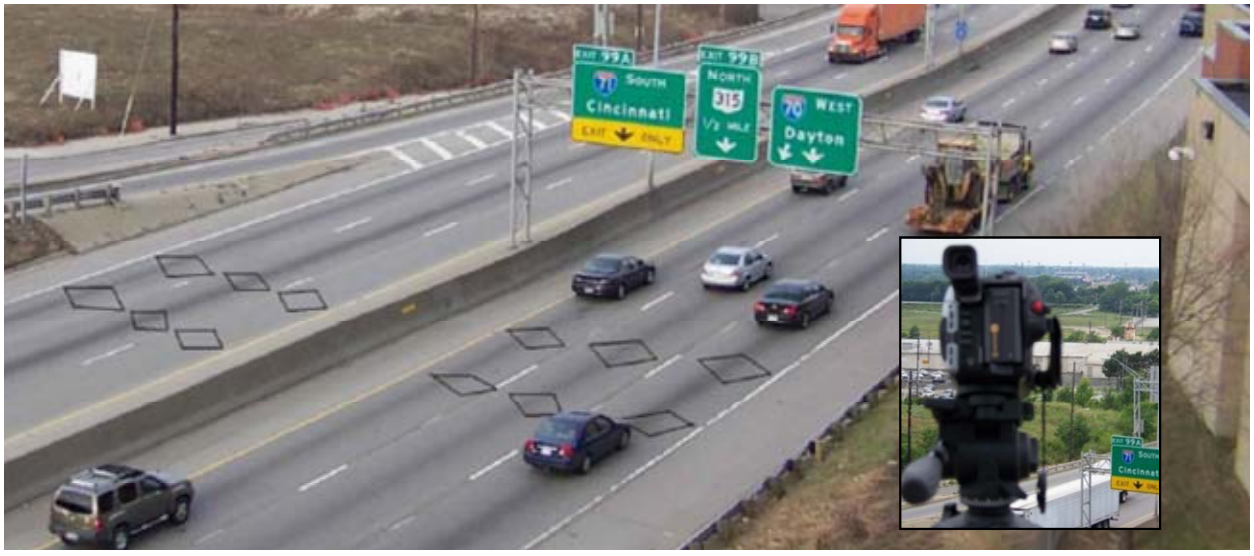

Figure 1. Video Data Collection at a Dual-Loop Detector Station in Columbus

The software VEVID enables to extract high-resolution vehicle trajectory data, such as timestamps on loops, speed, and vehicle length, from the videotapes, and it becomes possible to compare each estimated vehicle length with the corresponding real ones (Figure 2).

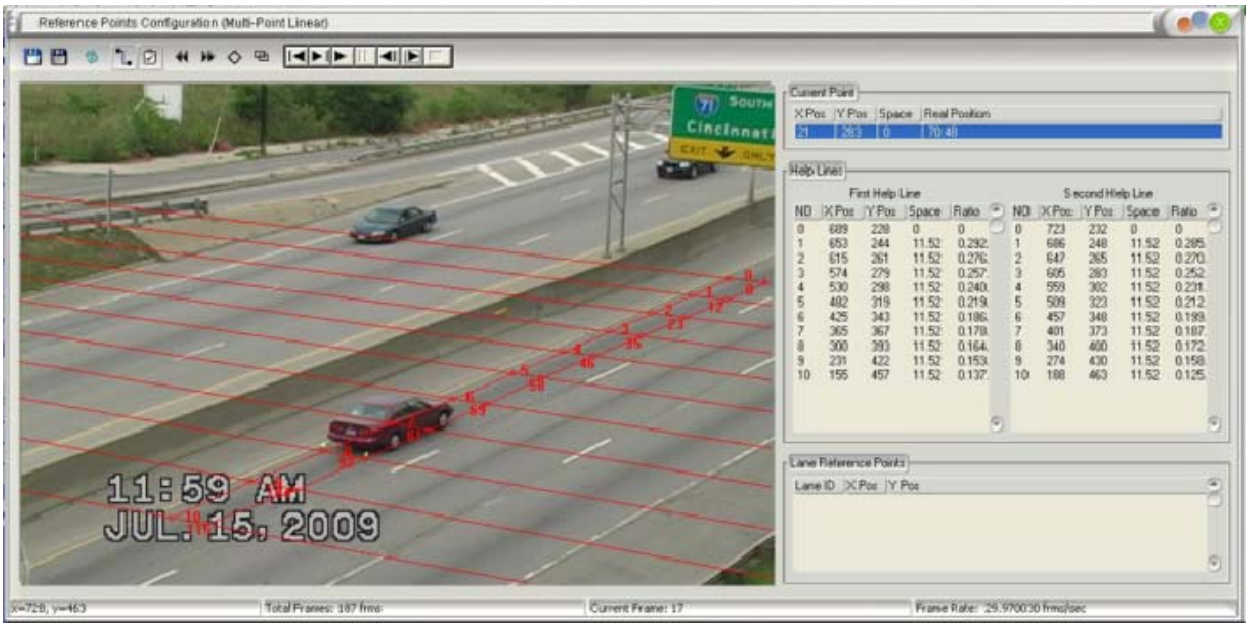

Figure 2. Using VEVID to Extract Vehicle Trajectory Data

Meanwhile, a probe vehicle equipped with a GPS traveler data logger is applied as a supplementary tool to collect traffic pattern data for validating parameters involved in the new models. A heuristic traffic state identification algorithm is developed to identify different traffic states, which ensures to use suitable models under a specific traffic state.

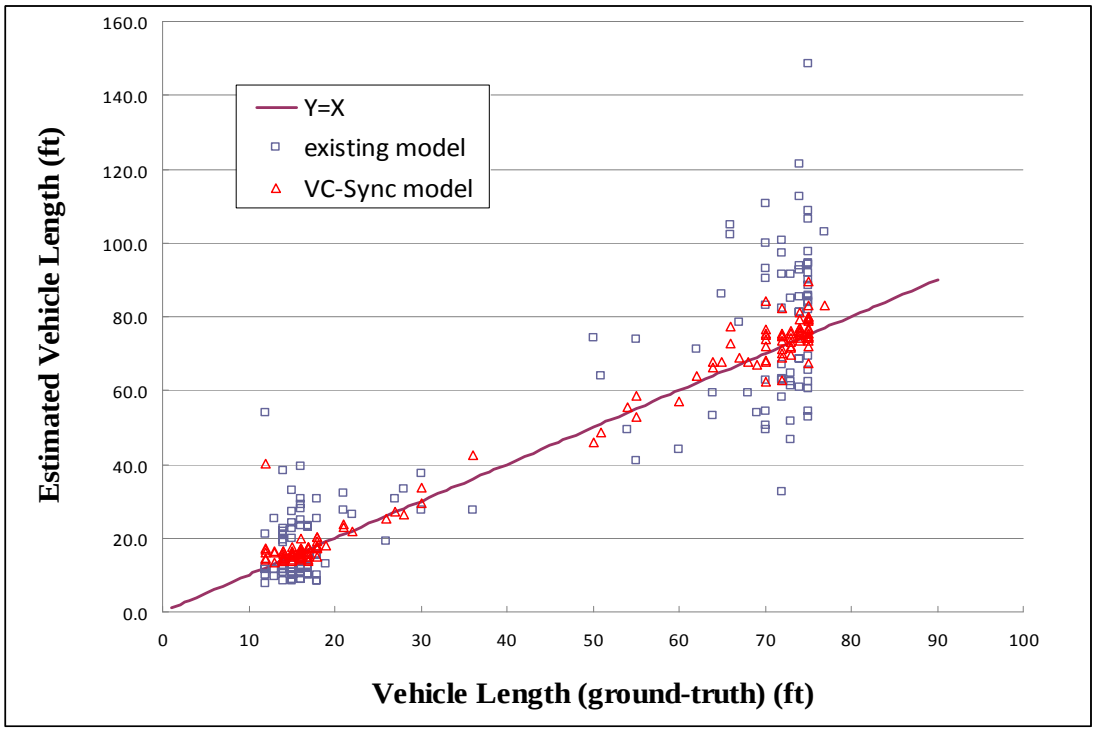

Figure 3. Outcomes of VC-Sync Model vs. the Existing Model

As a result, the Vehicle Classification model under Synchronized traffic (VC-Sync model) and the Vehicle Classification model under Stop-and-go traffic (VC-Stog model) are developed, respectively. Comparing to the obtained ground-truth data, it turns out that the error of the estimated length by the VC-Sync model is reduced to 8.5% compared to 35.2% produced by the existing model (Figure 3), and the error of the VC-Stog model is reduced to 27.7% compared to 210% generated by the existing model (Figure 4). This approach is also proven very cost-effective and applicable to practice.

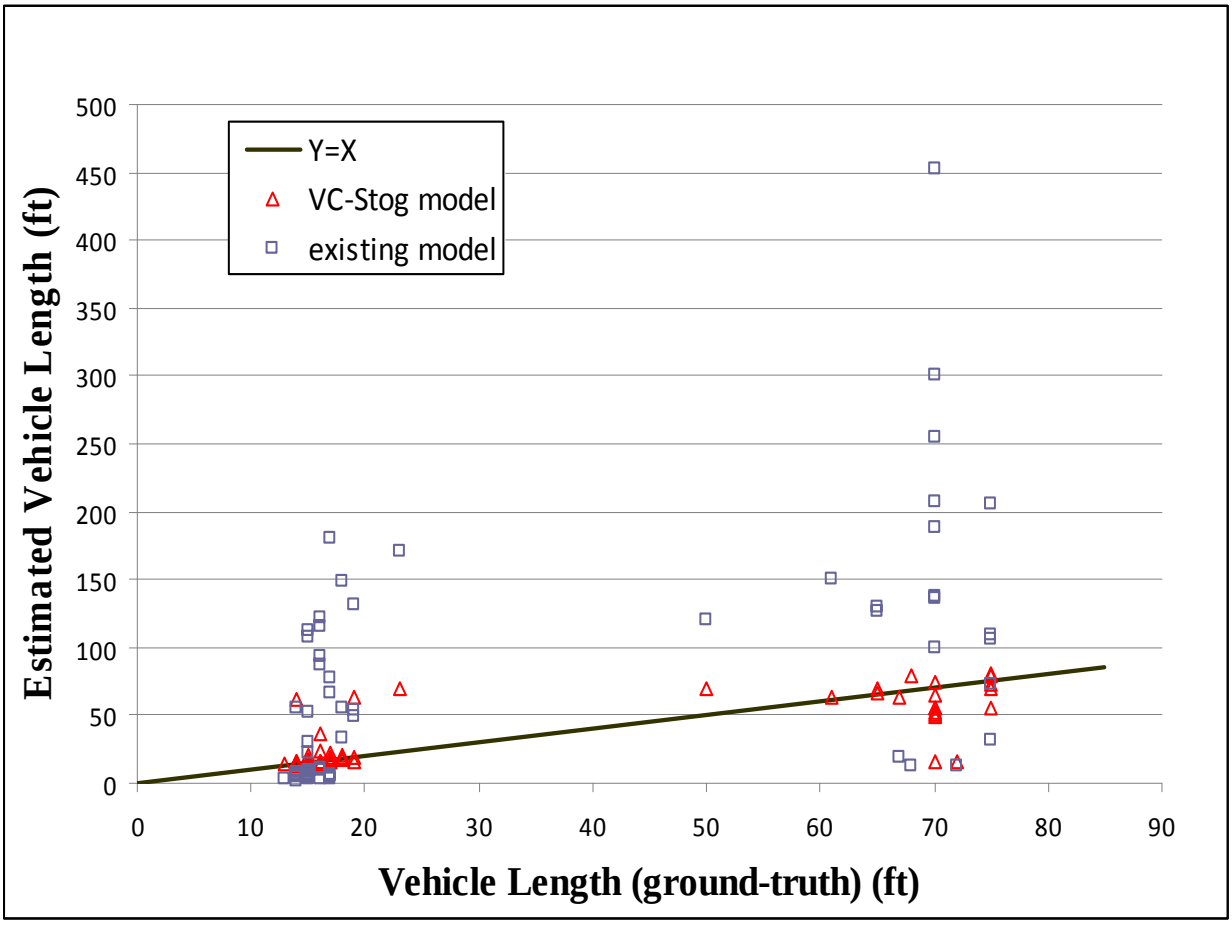

Figure 4. Outcomes of VC-Stog Model vs. the Existing Model

(The study presented in the abstract is supported by an OTC grant and advised by the author's advisor, Dr. Heng Wei, Associate Professor at University of Cincinnati. Tel: (513) 556-3781; Email: heng.wei@uc.edu)

Using Datamining in Classifications of Traffic Counting Locations: A Case Study in Ohio

Ramanitharan Kandiah
Assistant Professor, International Center for Water Resources Management, Central State University

John Davenport and André Morton
Undergraduate Students, Central State University

Introduction

On-Road Mobile Source Pollutants (ORMSP), such as carbon monoxide, nitrogen oxides and some hazardous air pollutants are induced by the transportation network. They can lead to breathing and heart problems, as well as issues with reproduction and even cancer in humans. Hence it is necessary to quantify the ORMSP amount and also to identify the hot spots in the routes. The classification and the ranking of the road segments can be looked into two ways; according to the Total Emission per Length of the road (TEL) and to the Total Emission per Segment (TES). The TEL classification can be used to evaluate the intensity of the ORMSP pollution along the transportation system, the TES classification can be used to identify the road segments according to their pollutant contribution.

This study explores a methodology to classify the routes with respect to the level of collective ORMSP emission. A case study is presented with Ohio highways traffic data.

Methodology

For each road segment, TEL is the metrics of all individual ORMSP emissions per length. Each TEL metric is computed as the product of actual emission of an ORMSP for a vehicle per mile and the number of the vehicles in the segment. TES for a segment is the metrics of all individual ORMSP emissions that is equivalent to the product of Vehicle Miles Traveled (VMT) and actual emissions of ORMSPs per mile. Here it is computed by multiplying TEL of the particular segment by the length of the segment. Once the TEL metrics and the TES metrics are computed for the transportation network, an unsupervised artificial neural network, Self Organizing Map (SOM) is used to classify the sections.

Self Organizing Maps

Self Organizing Map (SOM) has been extensively explored in many fields for the purposes of classification and pattern recognition (Kohonen, 2001). In SOMs, a competitive learning process is done only with inputs and without desired outputs. While the input layers are high-dimensional with the

original data the output layer neurons represent the reduced two dimensional data. An input layer neuron represents an input variable, and it is connected to each of the mapped output layer using a nonlinear projection. The data reduction is done through the iterative self-organization process; eventually, the input data is grouped into clusters. Extracted relationships can explain the system.

Two SOMs – one for TEL and the other for TES metrics- are developed using the metrics as the SOM inputs. Once the classifications are done, they are geographically visualized for further analysis.

Case Study

Annual Average Daily Traffic (AADT) count data for cars and trucks for three types of routes (state route, US route and interstate route) for six year period (2003-2007) in Ohio was obtained from ODOT. CO, PM and NO_x emissions per mile were assumed as those of the allowable emissions provided in Tier 2 standard (Diesel Net, 2010). TEL and TES metrics were computed in EXCEL. Classification was done with MATLAB – Neural Network toolbox. The final visualization was performed on ARCGIS.

Figure 1: Ohio Highway Network

Figure 2: Ohio-ORMSP Emission Levels

Results, Discussion and Conclusion

Considering the length, here only the TEL metrics based classification results are presented. The Based on TEL metrics, three distinct levels of on-road mobile pollution were identified along the Ohio

Highway network (Figure 2). While the entire interstate highway was in the highest emission group (Cluster 1), the sections of state highway routes and US highway routes fell into all three groups. It was found that the higher order pollution on US and state highways is released around the metropolitan areas in the state, and the collective ORMSAP emission per mile is higher in the northern region of Ohio than in the southern region of Ohio except in Cincinnati metropolitan area. ORMSAP pollutant hotspots were found around Cleveland, Columbus and Cincinnati metropolitan areas.

It has been demonstrated that the self organizing maps can be used to classify the transportation network based on the ORMSAP emissions. In the future, this approach can be improved by incorporating better individual pollutant emission estimates for a vehicle using programs like MOVES (EPA, 2010). Also, vehicles can be further categorized and additional ORMSAPs can be taken into account.

Acknowledgement

The authors thank the Ohio Transportation Consortium for financially supporting this study. We also want to thank Ohio Department of Transportation for providing the data.

References

Diesel Net Homepage: *Cars and Light-Duty Trucks—Tier 2*; See http://www.dieselnet.com/ standards/us/ld_t2.php (accessed September 2010)

Kohonen, T. *Self-Organizing Maps.* Springer, Berlin. 2001.

USEPA; *MOVES (Motion Vehicle emission Simulator).* U.S. Environmental Protection Agency; See http://www.epa.gov/otaq/models/moves/index.htm (accessed September 2010)

Studies of Novel Ceramic Materials as Precursors for Preparation of Ceramic-Metallic Composites for Lightweight Vehicle Braking Systems (Poster)

K. Myers and D. Loiacona
Youngstown State University

Corresponding Author:
Dr. Tim Wagner
Department of Chemistry, Youngstown State University

ABSTRACT

The title project centers on a close interaction between researchers in the YSU chemistry department and Fireline TCON, Inc. (FTi), which is a wholly-owned subsidiary of the Youngstown-based parent company Fireline, Inc. FTi has developed a unique process that transforms ceramic preforms into ceramic-metallic co-continuous interpenetrating phase composites with enhanced properties while retaining the original shape and dimensions of the preform. The TCON process offers enormous potential for cost-effectively producing materials for a wide variety of applications, including components for lightweight vehicle braking systems, which are of obvious benefit towards increased energy efficiency in vehicles. The primary goal of this project is to design, prepare, and investigate novel ceramic materials for use as precursors in the production of new TCON composites which meet or exceed specifications required for application as lightweight, high-strength, economical vehicle braking components.

Initial efforts are focusing on two systems: (1) nitrogen doped TiO_2 compounds, and (2) novel b-alumina related phases such as $SrTi_5Mg_6O_{17}$. These systems are designed to introduce Ti-Al and/or Ti-Al-Mg intermetallics into the final composite microstructure, which could have significant positive impacts on the properties useful for lightweight braking systems. Past attempts to incorporate TiO_2 into the TCON process have failed, due to poor wettability of TiO_2 in the reaction system. While very similar to pure TiO_2, the new $TiO_{2-x}N_x$ materials could have sufficiently different properties that they will more efficiently wet the system during the reaction to give desired product. The beta alumina phases are particularly interesting due to their potential for producing high strength nanocomposites on account of their crystal structures, which consist of open conduction channels separated by spinel blocks one nm thick. Initial data obtained for transformation of the known b-Alumina-like material, $SrMgAl_{10}O_{17}$, is shown in Figure 1.

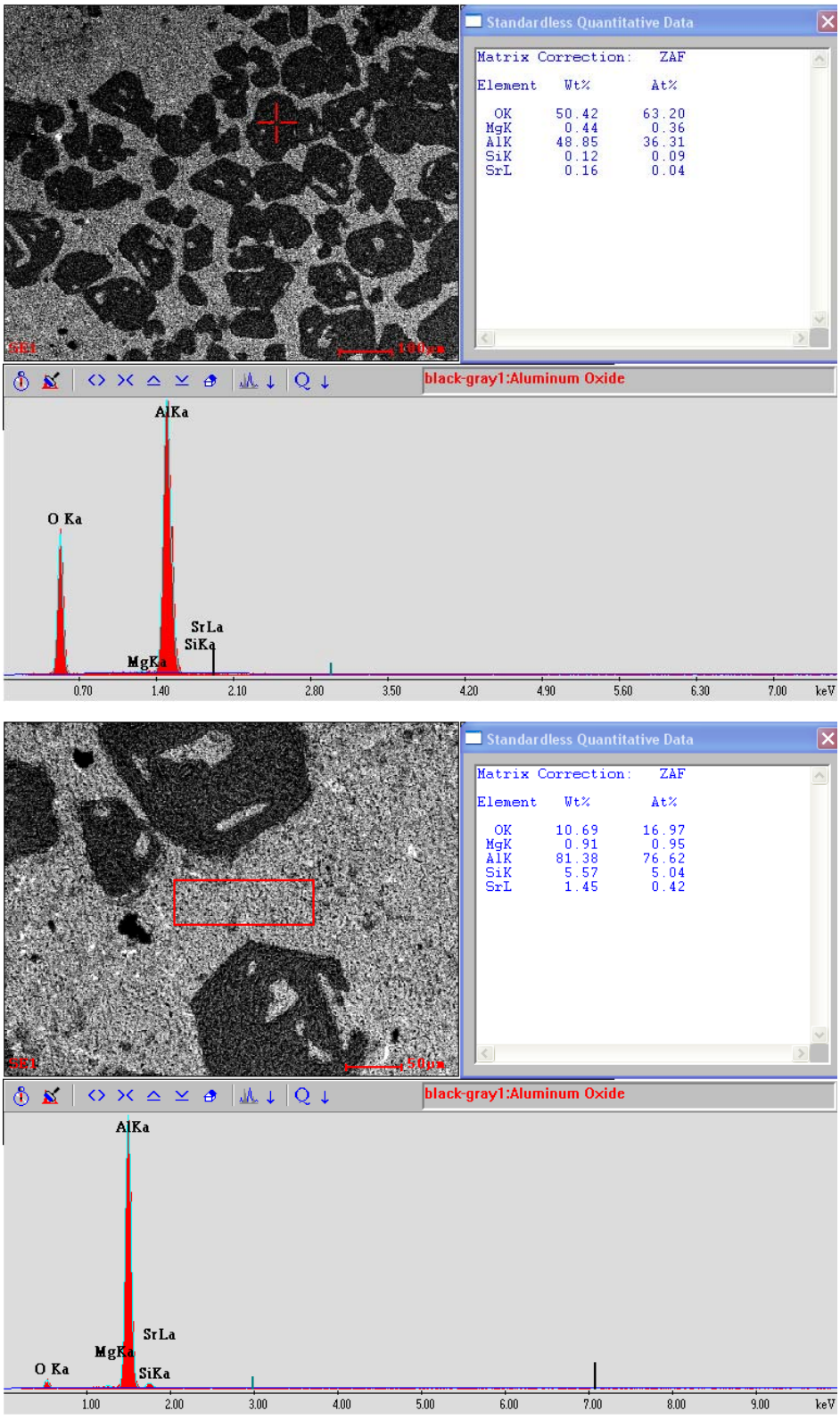

Figure 1: SEM /EDXS Data for $SrMgAl_{10}O_{17}$. Top and Bottom figures show EDXS results from the darker vs. lighter regions, respectively, verifying transformation to an Al-Al_2O_3 composite surface.